REPUBLIC OF TURKEY

ADANA ALPARSLAN TÜRKEŞ SCIENCE AND TECHNOLOGY
UNIVERSITY

GRADUATE SCHOOL OF NATURAL AND APPLIED SCIENCES
DEPARTMENT OF FOOD ENGINEERING

INVESTIGATION OF REBAUDIOSIDE A CRYSTALLIZATION
BEHAVIOR

SEMİH LATİF İPEK
MASTER OF SCIENCE

ADANA 2019

REPUBLIC OF TURKEY

ADANA ALPARSLAN TÜRKEŞ SCIENCE AND TECHNOLOGY
UNIVERSITY

GRADUATE SCHOOL OF NATURAL AND APPLIED SCIENCES
DEPARTMENT OF FOOD ENGINEERING

INVESTIGATION OF REBAUDIOSIDE A CRYSTALLIZATION
BEHAVIOR

SEMİH LATİF İPEK
MASTER OF SCIENCE

SUPERVISOR
ASSIST. PROF. DR. ALİ EMRAH ÇETİN

ADANA 2019

I hereby declare that all information in this thesis has been obtained and presented in accordance with academic rules and ethical conduct. I also declare that, as required by these rules and conduct, I have fully cited and referenced all information that is not original to this work.

Semih Latif İPEK

ABSTRACT

INVESTIGATION OF REBAUDIOSIDE A CRYSTALLIZATION BEHAVIOR

Semih Latif İPEK

Department of Food Engineering

Supervisor: Assist. Prof. Dr. Ali Emrah ÇETİN

September 2019, 67 pages

Stevia rebaudiana Bertoni is a source of more than 11 zero calorie sweet tasting compounds called steviol glycosides. These steviol glycosides especially Stevioside and Rebaudioside A (Reb A) which are two major glycosides found in the stevia leaves in higher amounts have received special interest for use as natural sweetener. The stevia extract should contain steviol glycosides at least 95 % in order to be used as a sweetener. Food and Drug Administration (FDA) approves the use of over 97 % pure Reb A in food products with a generally regarded as safe status (GRAS). The extraction, separation and purification of steviol glycosides are therefore crucial for the production of high purity natural sweeteners from stevia leaves.

Crystallization is one of the oldest and commonly used methods of industrial separation and purification. A compound of interest can be separated and purified from the extract by crystallization due to temperature and solvent dependent differences in the solubility values. Temperature and solvent dependent differences in the solubility values, the presence of supersolubility behavior and the growth of polycrystalline phases affect the separation/purification via crystallization. The aim of this thesis was therefore to determine temperature dependent solubility values and crystallization behavior of Reb A in water.

Thermodynamic solubility values of Reb A in water at 40, 50, and 60 °C were determined and found to be 3.94, 5.93 and 10.65 mg RebA/g water, respectively. Reb A was found to exhibit supersolubility and recrystallization in water. Particle morphologies were therefore determined by optical microscopy. Rounded and cornered shaped Reb A crystals was found to crystallize as thin and long whisker shaped crystals in water. X-Ray diffraction analysis also confirmed the crystallization of different Reb A phase from supersaturated solutions.

Solubility values of ground-water-grown-crystals were also determined at 20, 30, 40, 50 and 60 °C and found to be 0.55, 0.52, 0.70, 4.53 and 7.87 mg Reb A/g water.

Nucleation tresholds of Reb A were determined upon the observation of its supersolubility behavior in water. Primary and secondary nucleation tresholds of Reb A were determined both by holding Reb A solutions in constant temperature water bath and by isothermal crystal growth experiments in the glass double jacketed reactor under stirring at constant temperature. Reb A seeds were prepared for the determination of secondary nucleation tresholds. Primary nucleation thresholds were found to be between 0.0025 and 0.004 g/mL for 25 and 40 °C and between 0.004 and 0.01 g/mL for 50 and 60 °C by statically. Primary nucleation treshold determinations in stirred reactor however yielded 0.00399 g/mL and 0.00474 g/mL for 30 and 40 °C, respectively. Secondary nucleation tresholds by static system were found to be between 0.002 and 0.003 g/mL for 20 °C and between 0.004 and 0.003 g/mL for 30 and 40 °C. It was not possible to discriminate the secondary nucleation during isothermal crystal growth experiments either by visually or by spectrophotometric absorbance measurements within the solid liquid ratios employed and amount of seed suspension used.

Keywords: Stevia, Rebaudioside A, Solubility, Nucleation, Crystallization

ÖZET

REBAUDIOSIDE A'NIN KRİSTALİZASYON DAVRANIŞININ İNCELENMESİ

Semih Latif İPEK

Gıda Mühendisliği Anabilim Dalı

Danışman: Dr. Öğr. Üyesi Ali Emrah ÇETİN

Eylül 2019, 67 sayfa

Stevia rebaudiana Bertoni, steviol glikozitler adı verilen 11'den fazla sıfır kalorili tatlılık verici bileşiğin kaynağıdır. Bu steviol glikozitler, özellikle stevia yapraklarında daha yüksek miktarlarda bulunan iki ana glikozit olan Stevioside ve Rebaudioside A (Reb A), doğal tatlandırıcı olarak ilgi görmektedir. Stevia özütü, tatlandırıcı olarak kullanılabilmesi için en az % 95 oranında steviol glikozit içermelidir. FDA, ancak % 97'nin üzerinde saflığa sahip Reb A'nın gıda ürünlerinde kullanımını genel olarak güvenli statüsü (GRAS) ile onaylamaktadır. Bu nedenle steviol glikozitlerin ekstraksiyonu, ayrılması ve saflaştırılması, stevia yapraklarından yüksek saflıkta doğal tatlandırıcıların üretimi için çok önemlidir.

Kristalizasyon, en eski ve yaygın kullanılan endüstriyel ayırma ve saflaştırma işlemlerinden biridir. Söz konusu bir bileşik, sıcaklık ve çözücüye bağlı farklı çözünürlük değerleri sayesinde ekstrakttan kristalleştirilerek ayrılabilir ve saflaştırılabilir. Çözünürlük değerlerinde sıcaklık ve çözücüye bağlı farklılıklar, süper çözünürlük davranışının varlığı ve polikristalin fazlarının büyümesi, kristalizasyon yoluyla ayırma/saflaştırmayı etkiler. Bu nedenle bu tezin amacı, Reb A'nın su içerisindeki sıcaklığa bağlı çözünürlük değerlerini ve kristalizasyon davranışını belirlenmesidir.

Reb A'nın 40, 50 ve 60 °C'de su içerisindeki termodinamik çözünürlük değerleri belirlenmiştir ve sırasıyla 3.94, 5.93 ve 10.65 mg RebA/g su olarak bulunmuştur. Reb A'nın suda süper çözünürlük ve yeniden kristallenme davranışı gösterdiği bulunmuştur. Parçacık morfolojileri optik mikroskopi ile belirlenmiş ve yuvarlak ve köşeli Reb A kristallerinin, suda çözünerek ince ve uzun iğnecik şeklinde kristaller halinde kristallendiği bulunmuştur. X-Işını kırınımı analizi, farklı bir Reb A fazının, aşırı doymuş çözeltilerden kristalleştiğini doğrulamıştır. Suda

büyütülerek oluşturulan kristallerin öğütüldükten sonra çözünürlük değerleri 20, 30, 40, 50 ve 60 °C' de belirlenmiş ve 0.55, 0.52, 0.70, 4.53 ve 7.87 mg Reb A/g su olarak bulunmuştur.

Reb A'nın suda süper çözünürlük davranışı göstermesi sonucu nükleasyon eşiklerinin belirlenmesi amaçlanmşıtır. Reb A'nın birincil ve ikincil nükleasyon eşikleri, hem sabit sıcaklıkta su banyosunda hem de sabit sıcaklıkta karıştırmalı çift cidarlı cam reaktörde izotermal kristal büyüme deneyleri ile belirlenmiştir. İkincil nükleasyon eşiklerinin belirlenmesi içinse Reb A kristal çekirdekleri hazırlanmıştır. Birincil nükleasyon eşiklerinin statik sistemde 25 ve 40 °C' de 0.0025 ile 0.004 g/mL arasında ve 50 ile 60 °C' de 0.004 ile 0.01 g/mL arasında olduğu bulunmuştur. Bununla birlikte, karıştırmalı reaktördeki birincil nükleasyon eşik değerleri, sırasıyla 30 ve 40 °C' de 0.00399 g/mL ve 0.00474 g/mL olarak bulunmuştur. Statik sistemde ikincil nükleasyon eşik değerlerinin 20 °C için 0.002 ile 0.003 g/mL arasında ve 30 ve 40 °C için 0.004 ile 0.003 g/mL arasında olduğu bulunmuştur. İkincil nükleasyonun kullanılan katı sıvı oranları ve çekirdek süspansiyonu miktarı değerleri çerçevesinde izotermal kristal büyümesi deneyleri ile görsel olarak veya spektrofotometrik absorbans ölçümleriyle ayırt edilmesi mümkün olamamıştır.

Anahtar Kelimeler: Stevia, Rebaudioside A, Çözünürlük, Nükleasyon, Kristalizasyon

To my family

ACKNOWLEDGEMENTS

TABLE OF CONTENTS

LIST OF FIGURES

LIST OF TABLES

NOMENCLATURE

PSD   Particle Size Distribution

Reb A   Rebaudioside A

WHO   World Health Organization

FAO   Food and Agriculture Organization of the United Nations

1. INTRODUCTION

1.1. Stevia

Consuming low-calory sweeteners rather than high calorie sugars has been increased over the last years due to increasing concern against some health problems like obesity and diabetes stemming from unbalanced nutrition. Having almost zero calorie, *Stevia rebaudiana* Bertoni plant came into prominence in sweetener industry as its natural structure and other beneficial properties. It is a perennial shrub which is native in Paraguay and some areas of adjacent countries. It has been known for ages by indigeneous people and used as folk remedy by these people for various aims. In modern era, it was discovered in early 20th century and classified in modern literature. Then its cultivation spreaded over the World. Stevia has attracted much interest over the world for different purposes. Stevia plant is famous for its intense sweet taste. Besides its intense sweetness, its glycosides have not carcinogenic, mutagenic and tetratogenic effects. It has a high potential to be used as substitute saccharose. Stevia and its related glycosides have also health beneficial properties like anti-hyperglycemic, anti-hypertensive, anti-inflammatory, anti-tumour, anti-diarrhoeal, diuretic, and immunomodulatory effects. They also help treat diabetes mellitus, obesity, hypertension and caries prevention. Stevia products are extensively used in over the World. Japan was the first country to use stevioside in soft drinks in 1970s. Since then, Stevioside and Reb A extracted from Stevia leaves have been used in a variety of products. The source of sweet taste is steviol glycosides in stevia leaves. There are more than 11 steviol glycosides having 50-500 times sweeter taste than sucrose with zero calorie depending on type of steviol glycoside (Lemus-Mondaca, Vega-Gálvez, Zura-Bravo & Ah-Hen, 2012; Wölwer-Rieck, 2012). Steviol glycosides in stevia leaves is given in Table 1.1.

In the center of steviol glycoside molecules, there is an aglycone called ''steviol'' (Figure 1.1). The number of carbohydrates binding to steviol or the type of bonding defines the steviol glycoside. Reb A and stevioside are the most abundant glycosides in stevia leaves. Despite having higher amount in stevia leaves than Reb A, stevioside has a bitter after taste (Lemus-Mondaca et al., 2012).

Table 1.1. Steviol Glycosides in Stevia Leaves (Puri, Sharma & Tiwari, 2011; Prakash, Markosyan & Bunders, 2014).

Glycoside	Molecular Formula	Molecular Weight (g/mol)	Rate in the Leave (%)
Rebaudioside A	$C_{44}H_{70}O_{23}$	967.01	2.0 - 4.0
Rebaudioside B	$C_{38}H_{60}O_{18}$	804.88	<< 1.0
Rebaudioside C	$C_{44}H_{70}O_{22}$	951.01	1.0 - 2.0
Rebaudioside D	$C_{50}H_{80}O_{28}$	1129.15	<< 1.0
Rebaudioside E	$C_{44}H_{70}O_{23}$	967.01	<< 1.0
Rebaudioside F	$C_{43}H_{68}O_{22}$	936.99	<< 1.0
Rebaudioside M	$C_{56}H_{90}O_{33}$	1291.3	
Stevioside	$C_{38}H_{60}O_{18}$	804.88	5 – 10
Steviolbioside	$C_{32}H_{50}O_{13}$	642.73	<< 1.0
Rubusoside	$C_{32}H_{50}O_{13}$	642.73	
Dulcoside A	$C_{38}H_{60}O_{17}$	788.87	0.4 – 0.7
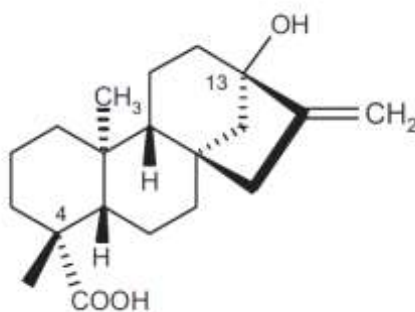
Figure 1.1. Steviol (Brahmachari, Mandal, Roy, Mondal & Brahmachari, 2011).
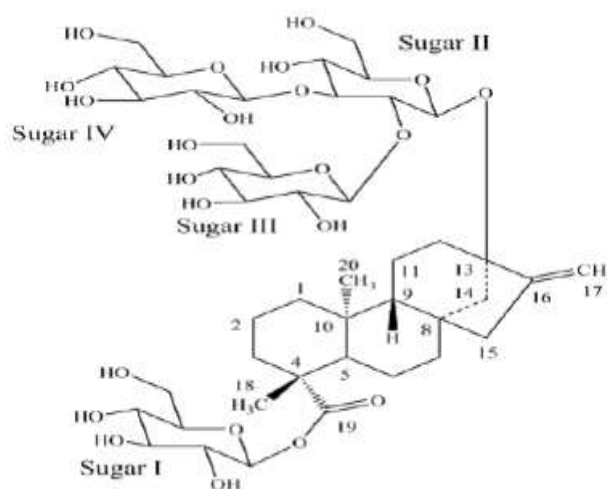
Figure 1.2. Rebaudioside A (Prakash et al., 2014).

Reb A has a four glycose molecule bond to hydroxyl group of 13th and 19th carbons of steviol molecule. Three glucose molecules are bond to hydroxyl group of 13th carbon atom whereas one glucose molecule is bond to hydroxyl group of 19th carbon molecule. This is why Reb A is sweeter than stevioside as stevioside has three glucose molecules (Figure 1.2).

For commercial use, total steviol glycoside extract is produced by extraction and then dried. The Joint FAO/WHO Expert Committee on Food Additives" (JECFA) specified that at least 95 % of stevia extract should be composed of steviol glycosides in order to be used as natural sweetener (FAO/WHO, 2017). American Food and Drug Administration institute gave GRAS "Generally regarded as safe" (GRAS Assessment, Layn Corp, 2010) status to Reb A on condition that it should have a purity at least % 97. Production of high-purity single steviol glycoside requires separation and purification. In this respect, solubility values and crystallization conditions are of critical importance. Water and ethanol, methanol or their mixtures are generally used for extraction process. Reb A is more soluble in water than stevioside therefore hot water is mostly used as medium in extraction process (Abou-Arab, Abou-Arab & Abu-Salem, 2010).

The purification diagram of Reb A is given in Figure 1.3. The solubilities of steviol glycosides in water or ethanol at various temperatures determine their extraction efficiencies. Crystallization is used for the purification of Reb A. Reb A however exhibit polymorphism depending on the solvent used during the extraction and purification (Prakash, DuBois, Clos, Wilkens & Fosdick, 2008; Upreti, Smit, Hagen, Smolenskaya, & Prakash, 2012). Amorphous, anhydrous, solvated and hydrrated crystal phases of Reb A have been reported (Prakash et al., 2008; Upreti et al., 2012). Crystallization is the most popular method for purified solid material production in industry. More than % 90 of solid compounds are purified and produced in all industries (Gao, Rohani, Gong & Wang, 2017). For organic materials, crystallization from solution is mostly preferred. However, the lack of solubility data in literature hinders a fast process design in the industrial practice. Temperature dependent solubility values in various solvents is the primary driving force in the separation and purification of a substance. Supersolubility, polymorphism, crystal growth and metastable crystal transformations contribute to the crystallization process. The supersolubility behavior and the presence of metastable region neccessitates the determination of primary and secondary nucleation tresholds for the controlled growth of crystals. The aim of this thesis

was therefore to determine water solubilities of Reb A at different temperatures and to investigate its crystallization behavior in water.
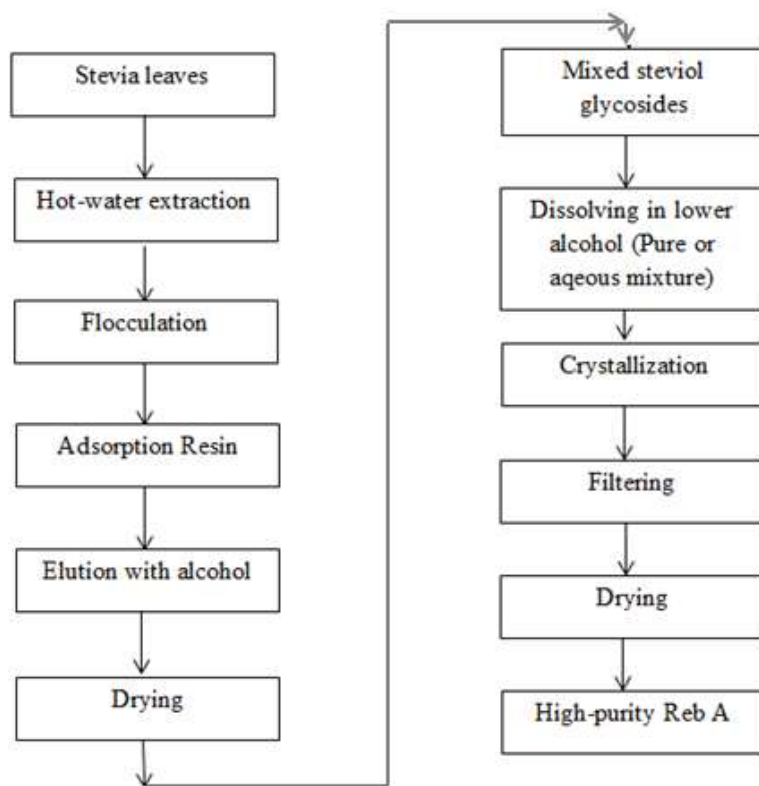
Figure 1.3. Purification diagram of Reb A (Prakash et al., 2008).

2. LITERATURE REVIEW

2.1. Crystallization

Crystallization is one of the oldest methods of purification and separation in both industrial and scientific purposes. Approximately % 90 of commerical active pharmaceutical ingredient products are produced as organic crystals and crystallization process is the key process in determining the final product quality of these products (Gao et al., 2017). The crystallization is also used in the production of a wide variety of products besides active pharmaceutical ingredients. Beyond being a method used only in the production of products, crystallization is a process that affects downstream processes such as filtering, drying, grinding (Alvarez & Myerson, 2010). Crystallization has a wide range applications in food industry. The substances such as sugar, salt and lactic acid are produced and purified as crystals (Berk, 2018). Many substances that are not desired in the food are also separated by crystallization (winterization in oils, etc.).

Crystallization is defined as the formation of solid crystals from the liquid (Mersmann, 2001; Hartel, 2001; Decloux, 2002; Berk, 2018) or the formation of an amorphous solid (Jouppila & Roos, 1994; Berk, 2018). Crystallization from solution is more commonly used in the separation of the pharmaceuticals and some organic molecules than superciritical and melt crystallization (Tung, Paul, Midler, & McCauley, 2009). Crystallization from solution is performed by making solution supersaturated with respect to compound of interest at a certain temperature (Berk, 2018). The crystallization process in solution takes place in two phases at supersaturation conditions; nucleation and crystal growth (Berk, 2018). Characteristics of the solvent and solubility of the solute should be well known and investigated for the crystallization process.

2.2. Solubility

Determination of solubility behaviour and characteristics of a substance is an integral part of a successful crystallization process. How much a solvent can dissolve a certain substance at a given temperature is of importance in the preparation of the solutions in the crystallization processes before the process begins and to know how much undissolved material remains in the solution at the end of the process (Myerson, 2001). Each liquid has maximum solubility limit of a corresponding solid at a certain temperature. When this limit is exceeded, the

solution becomes saturated. The maximum amount of solids that can be dissolved to saturate a liquid at a certain temperature gives the solubility of the solid in that liquid (Myerson, 2001). While the solution is in a saturated state, it cannot dissolve any more matter and the solution is at equilibrium (Figure 2.1). After this step, the added solids settle to the bottom and the concentration in the solution do not change (Tung et al., 2009). The effect of pressure is low therefore the effect of pressure on the solubility is generally ignored (Beckmann, 2013). There are three methods to express solutions mathematically; weight percent (grams solute in 100 grams solution), mass or mole fraction (grams solute/grams solution or mole solute/mole solution), grams solute per volume solution or solvent. If volume is to be used in calculations, density of solvent should be taken into consideration at corresponding temperatures. Calculations using mass or mole fractions give easier and more accurate results (Beckmann, 2013; Myerson, 2001). Solubility is a temperature dependent property. The amount and strength of the solubility vary from substance to substance and mostly increase with temperature rise. There are some exceptions such as calcium hydroxide and sodium chloride. Calcium hydroxide solubility decreases with increasing temperature. Temperature has a weak effect on the solubility of NaCI. This reveals the necessity of knowing the specific solubility characteristics of each substance for the separation and purification via crystallization.
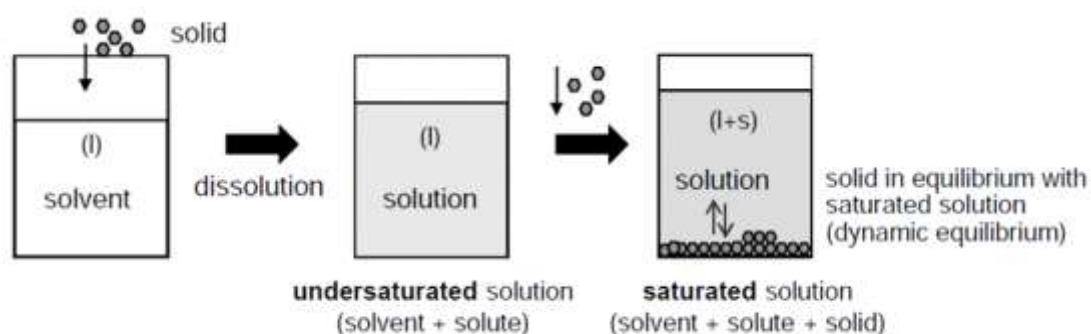
Figure 2.1. Solution equilibrium (Beckmann, 2010).

2.2.1. Thermodynamic definition of solubility

Free-energy composition diagram is used to examine the solubility. The following diagram represents the Gibbs free energy profile of a binary system. The y-axis shows the Gibbs free energy of the system and the x-axis shows the mass fraction. The first component is the solid and the second is the solvent. Temperature and pressure are considered constant.

According to Figure 2.2, there are two scenarios. The first scenario (Curve 1) is concave upward. This means that the Gibbs free energy of the binary mixture present in any composition is lower than the only constituent of the mixture. It is more stable than the constituents alone. This solution is therefore considered as a single-phase. Mathematically concave shape can be expressed as follows;

$$G < 0 \; and \; \frac{\partial^2 G}{(\partial x)^2} > 0 \qquad (1)$$
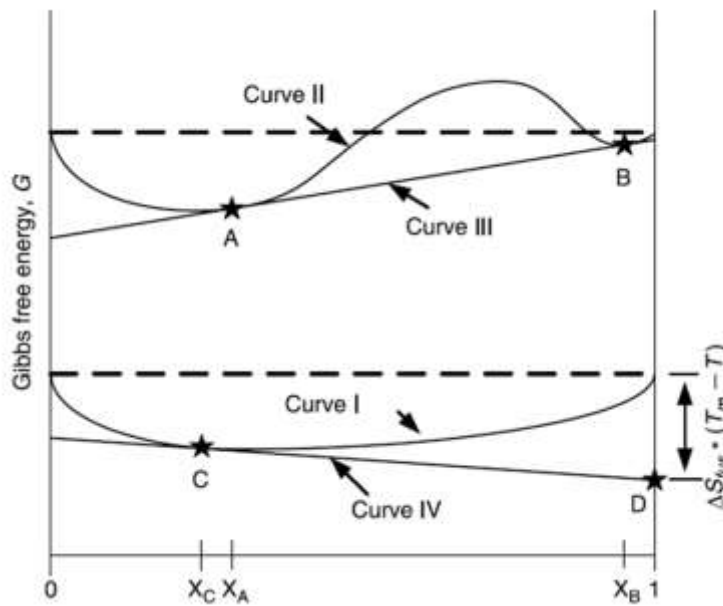
Figure 2.2. Equilibrium in a binary system (Tung et al., 2009).

The second scenario is the points A and B shown in the Figure 2.2. Curve 2 consists of two up and one down concave. The points A and B are the tangent lines on the y axis representing the compositions in the range from 0 to 1 and are the intersection points with the Curve 2. At these points, the Gibbs free energies are identical, no matter how much the solvent and the solute are mixed. In other words, they are in equilibrium at points A and B. Point A represents solvent and solute mixtures while point B represents the solvent-containing oil or amorphous solid. These two points are called the free energy diagram binodal points. When the fraction is below the point A, the mixture is undersaturated, when it rises above A the mixture is supersaturated (Tung et al., 2009).

The liquid-solid equilibrium is explained by the Curve 4 and the Curve 1 in intersection C point (equilibrium resolution) and the D point (crystal equilibrium point).

$$\mu(solid\ phase) = \mu(liquid\ phase \tag{2}$$

$$= \mu(pure\ compound\ as\ liquid\ at\ temperature\ T) + RT \cdot ln\alpha$$

or equivalently

$$ln\alpha = lnx_i^{SAT} \cdot \gamma_i^{SAT} = \frac{\Delta_{fus}S}{R}(1 - \frac{T_m}{T}) \tag{3}$$

where μ is the partial molar Gibbs free energy, T is the temperature, T_m is the melting point of the compound, R is the Boltzman constant, ΔS is the entropy of fusion, α is the activity of the compound of interest in solution, which is directly related to the amount of compound dissolved, i.e., solubility lnx_i^{SAT}, and activity coefficient γ_i^{SAT}. These two formulas show that temperature, difference in the chemical potential of a compound as a solid and a liquid, or entropy of melting can directly affect solubility. In addition, the solvent and impurities affect the activity coefficient. The chemical structure of the compound and the salt forms affect the melt entropy and the activity coefficient of a substance and hence its solubility (Tung et al., 2009).

2.2.2. Ideal and Non-Ideal Solutions

The ideal solution is considered to be the solution in which the interactions between the solute and the solvent are identical (Mullin, 2001). Despite it is impossible to practice, ideal solutions are used as reference for other solubility calculations. The solubility of ideal solutions is estimated mathematically from the van't Hoff equation (Mullin, 2001);

$$lnx = \frac{\Delta H_f}{R}\left[\frac{1}{T_f} - \frac{1}{T}\right] \tag{4}$$

where x is the mole fraction of the solute in the solution, T is the solution temperature (K), T_f is the fusion temperature of the solute (K), ΔH_f is the molal enthalpy of fusion of the solute (J mol^{-1}) and R is the gas constant (8.314 Jmol^{-1}K^{-1}).

By using this formula, the solubility curve of a substance can be ideally drawn, but mostly these curves are unjustified since no specific reference substance is used. It can also be expressed as;

$$lnx = -\frac{\Delta H_f}{RT} + \frac{\Delta S_f}{R} \tag{5}$$

$\Delta H_f = T_f \Delta S_f$. ΔS_f is the molal entropy of fusion. If the solution exhibits non-ideal behavior, it may give a different curve than $-\Delta H_f/R$ even if the T^{-1} curve versus lnx exhibits a smooth line. In such cases, the enthalpy and entropy of mixing must be taken into account by replacing ΔH_f with ΔH_d (of dissolution) and ΔS_f by ΔS_d (Beiny and Mullin, 1987; Mullin, 2001);

$$lnx = -\frac{\Delta H_d}{RT} + \frac{\Delta S_d}{R} \tag{6}$$

Another approach is the calculation of the change in Gibbs free energy of the mixtures. The enthalpy and entropy changes in solutions are expressed as follows;

$$\Delta G = \Delta H - T\Delta S \tag{7}$$

If the solution is an ideal solution, the formula is shown as follows;

$$\Delta G = RTlnx \tag{8}$$

x in the above equation represents one of the compounds present in the solutions. The entropy change accompanies this dissolution process using following equation.

$$\Delta S = -Rlnx \tag{9}$$

The enthalpy of mixing, ΔH, is zero for an ideal solution. General energy change can be expressed in terms of activity coefficient. Assuming that α is one of the compounds;

$$\Delta G = RTln\alpha \tag{10}$$

In ideal solutions;

$$\alpha = x \tag{11}$$

Activity coefficient should be used in non-ideal solutions;

$$\alpha = \gamma x \tag{12}$$

In this case the formula can be expressed as follows;

Schroder-van Laar equation;

$$\ln(x\gamma) = \frac{\Delta H_f}{R}\left[\frac{1}{T_f} - \frac{1}{T}\right] \tag{13}$$

The key to the use of equation for the prediction of solubilities in non-ideal systems is reliable estimation of the activity coefficient γ. In non-ideal solutions, the basis of using the above

formula is to use the correct activity coefficients. The correct coefficients should be obtained and used to calculate the solubility of organic solids in organic solvents (Mullin, 2001).

2.2.3. Solubility of Inorganic and Organic Materials

Although the structure of the substances are similar, their solubility can vary considerably (Mullin, 2001). NaCl is observed to have a relatively weak temperature dependence with the solubility varying between 35.7 and 39.8g/100g water over a 100 °C range. However, solubility of potassium nitrate varies between 13.4 and 247g/100g water over the same temperature range (Myerson, 2001). Despite a wide range of difference, salts in general have high degree of solubility (Beckmann, 2013). There are exceptions like calcium hydroxide as its solubility decreases with increasing temperature (Myerson, 2001). Inorganic compounds may have hydrate forms which affect the solubility. For solubility and crystallization calculations, the hydrate form must be included in the process. The solubility values of organic substances in water, many organic solvents and their mixtures with water in varying percentages hold significant importance in the crystallization of organic substances (Myerson, 2001).

2.2.3.1. Solubility of Inorganic Materials

The solubility of inorganic compounds commonly deals with inorganic matter – water systems. Although solubility of a compound is related to its own chemical structure, temperature may increase or decrease the solubility. In some cases solubility of a compound such as NaCI is independent of temperature (Beckmann, 2013). Temperature vs. solubility curve therefore may not be always straight. After a point during temperature rise, the solubility curve can be reduced. There may be a phase change at these points as it is seen for sodium sulphate which crystallizes in the form of decahydrate (glauber salt) at low temperatures but it forms anhydrate over 32.4°C.

The basic principle of obtaining the solubility curves comes from the Le Chatelier's principle. The ionic bonds of the ionic salt crystals are broken down and the formation of weak electrostatic ion - dipole interactions due to hydration is taken into consideration. Temperature dependence of solubility in ideal solutions can be predicted by using Schröder van Laar equation stated above. Figure 2.3 show the temperature dependence of the solubility (Beckmann, 2013).
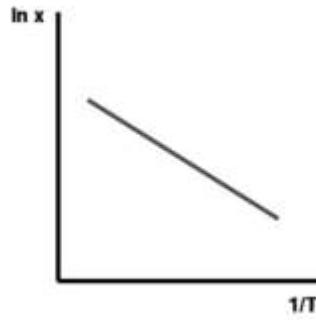
Figure 2.3. The temperature dependence of the solubility (Beckmann, 2013).

2.2.3.2. Solubility of Organic Materials

The solubility of organic substances in water, various organic solvents and their mixtures are also important. Considering the fact that the most of the substances produced in the food and pharmaceutical industries are organic substances, the determination of solubility is crucial. Due to the limited nature of solubility data in the literature it is difficult to determine the accurate solubility values by mathematical calculations. In this respect, the solubility should be determined in the most appropriate way by considering the effects of factors such as temperature, pressure, chemical properties and the impurities.

According to Myerson (2001) the balance between solvent and solute shown as;

$$\mu_{i_{solid}} = \mu_{i_{solution}} \tag{14}$$

$$x_2 = \frac{f_{2_{solid}}}{\gamma_2 f_2^0} \tag{15}$$

x_2 denotes the mole fraction of the solute in the solution. γ_2 represents the activity coefficient of the solute. f_2^0 is the standard state fugacity. The above equations give the solubility of any solute in any solvent. It is inferred from these equations that the solubility coefficient is related to fugacity ratio. Fugacity is normally used for the solvent in the super-cooled liquid below freezing point. In this case, vapor pressures are used in place of fugacity. The solute and solvent have low vapor pressures. In this case, when the solvent and solute are similar in structure the ideal solubility equation becomes:

$$x_2 = \frac{P^S_{2_{solid\ solute}}}{P^S_{2_{subcooled\ liquid\ solute}}} \tag{16}$$

11

The ideal solubility depends on the solvent and not the solute, the chemical differences between the pure substance phase change the triple point and consequently the ideal solubility (Prausnitz, Lichenthaler & Gomes de Azevedo, 1999). A pure component phase diagram is given in Figure 2.4.
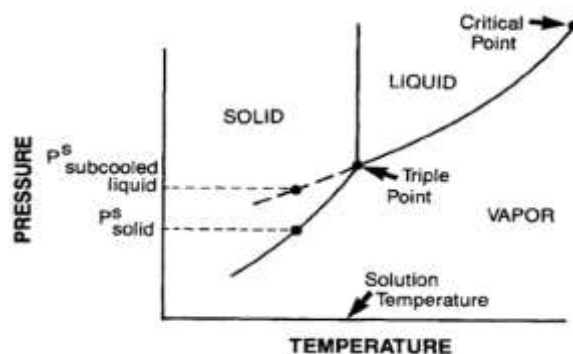
Figure 2.4. Extrapolation of liquid vapor pressure on a pressure temperature diagram for a pure material (Prausnitz et al., 1999).

The ideal solubility of the substances can be easily calculated by

$$x_2 = \exp\left[\frac{\Delta H_m}{R}\left(\frac{1}{T_m} - \frac{1}{T}\right)\right] \tag{17}$$

T_m is the normal melting temperature. R denotes the gas constant. Details can be found in Myerson (2001). The different isomers of some substances may have an ideal solubility which is very different from each other. The rate of increase in solubility also varies depending on the heat of fusion. Lower heat of fusion means higher solubility. The above formula does not provide any information about the solvent-solute relationship or solvent, although it is easier to compare the solubility of solutes. For this reason, activity coefficients must be calculated.

Although the solubility of organic molecules is very important in industry, the solubility data in the literature may be limited. The prediction of solubility is somewhat complicated if the solubilities of an organic molecule in many solvents or their mixtures need to be determined. There are two ways to determine the solubility of an organic solute; prediction or experimentation. Mostly, despite the need for experimentation, sometimes the prediction is sufficient. Determination of the solubility of organic substances in mixed solvents is also of particular importance. It is a long and laborious task to obtain experimental data for various solvent ratios.

2.2.4. Measurement of Solubility

The basis of a good crystallization design is to obtain accurate solubility data. Since the solubility values in the most of the non-aqueous or multiple solvent mixtures may not be available in literature and the accuracy of the mathematical estimation of the solubility is not known, solubility experiments are carried out in laboratory environment. However, the solubility experiments are prone to personal errors in every stage. According to Myerson (2001), solubility experiments should be performed under certain conditions in order to minimize these errors. It is necessary to ensure constant temperature and a stirred environment. Constant temperature should be ensured by jacketed heaters. The mass of the solvent should be known. If the temperature of solvent is higher than room temperature or organic solvent is used, the cooling column should be attached to the system in order to avoid solvent loss due evaporation. Pure phase solute should be added into the solvent and solute and solvent should be incubated for at least 4 hours, preferably 24 hours at desired temperature. Samples should then be taken for analysis. Dissolution may be a long-lasting process to reach saturation. For this, the values obtained as a result of waiting for 1 hour and under will be less and incorrect.

2.2.5. Supersolubility

Crystallization is a process performed at specific conditions (temperature, pH, concentration) and it is time-dependent. A driving force is needed to achieve crystallization. This driving force in crystallization is supersaturation. Supersaturation is the dissolution of the solid in the amount higher than the equilibrium concentration in the solution at specific temperature. In order to achieve the crystallization process, solution must converted into supersaturated state with respect to solute by certain methods. The cooling method is the most commonly used method to supersaturate solutions (Mersmann, 2001). Mathematically, the supersaturation is expressed as (Rashid, 2011).

$$s = C - C^*$$
(18)

s is the supersaturation, C denotes the actual concentration of solute in solution, and C^* is the equilibrium concentration. Supersaturation ratio and relative supersaturation are commonly used terms (Rashid, 2011). Supersaturation ratio is calculated as follows:

$$S = \frac{C}{C^*}$$
(19)

It is expressed as and is always greater than 1 for supersaturated solutions. Relative supersaturation (σ) is achieved by subtracting 1 from supersaturation ratio (S);

$$\sigma = \frac{C}{C^*} - \frac{C^*}{C^*} = \frac{s}{C^*} = S - 1 \tag{20}$$

The definition of supersaturation can vary according to the crystallization mechanism. If the rate limiting step is mass transfer, generally the Equation 18 is used. The Equation 19 is used in the theoretical nucleation models. If the rate limiting step is surface integration, the Equation 20 is preferred (Rashid, 2011).

2.2.6. Nucleation and Metastable Zone Width

Nucleation is the formation of new embryonic crystals without the addition of any seed in a supersaturated medium. It is impossible to have nucleation in undersaturated environments. Nucleation is however inevitable in labile environments. There is such a region on the solubility curve that the solution is supersaturated and no or negligible nucleation occurs but crystal growth takes place. This region is called metastable zone and all crystallization processes are performed in this region. Before industrial batch crystallization processes, metastable zone width should be determined accurately. The purpose of the crystallization process is to perform a crystallization process to ensure production of crystals in similar sizes and quality. Controlled crystallization can only be performed within the metastable zone since only crystal growth occurs in this zone. Two standard methods are available to determine the metastable zone width. The first one is the polytermal method, the solution is cooled until the visible crystals forms. The second method is isothermal method. In this method, a supersaturated solution is prepared and stirred at constant temperature and nucleation in the solution is determined. From the first moment when the supersaturation occurs, the time until the crystals appear is called induction time. In the diagram below (Figure 2.5), the zones in which the crystallization occurs or does not occur are expressed depending on the concentration and temperature. The formation of embrionic crystals in the labile environment is called primary nucleation and can occur only on and above the primary nucleation curve. Primary nucleation occurs homogeneously or heterogenously. Homogenous primary nucleation is the nucleation that occurs without any foreign substance or without any surface contact. Although it has very little industrial practice, it is the starting of nucleation theory. Primary nucleation in the presence of foreign matter or by surface contact is called as heterogenous nucleation. The theory of primary nucleation can be found in (Mullin, 2001;

Rashid, 2011). According to this theory, atoms in the solution come together to form clusters. Figure 2.5 shows a schematic diagrams of solubility-supersolubility (Miers and Isaac, 1906; Miers and Isaac, 1907; Rashid, 2011).
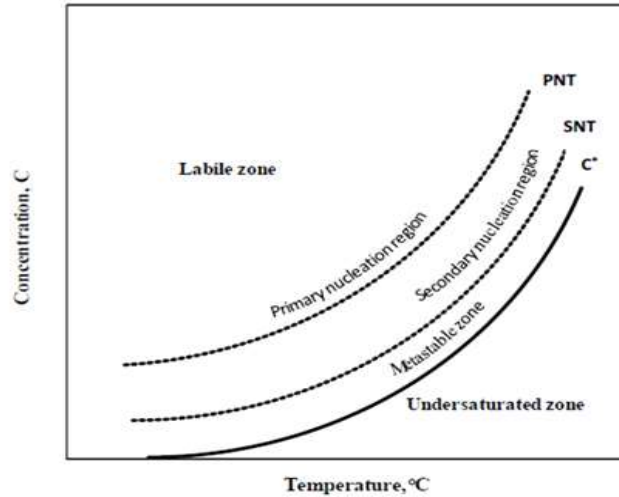
Figure 2.5. A schematic diagram of solubility-supersolubility (Miers and Isaac, 1906; Miers and Isaac, 1907; Rashid, 2011).

The formation of cluster and embryos leading to tghe formation of nucleus in solution can be expressed by following reactions:

$$
\begin{aligned}
\alpha + \alpha &\leftrightarrow \alpha_2 \\
\alpha_2 + \alpha &\leftrightarrow \alpha_3 \\
\alpha_3 + \alpha &\leftrightarrow \alpha_4 \\
&\ldots\ldots\ldots\ldots \\
&\ldots\ldots\ldots\ldots \\
\alpha_{m-1} + \alpha &\leftrightarrow \alpha_{m(critical\ cluster)}
\end{aligned}
\tag{21}
$$
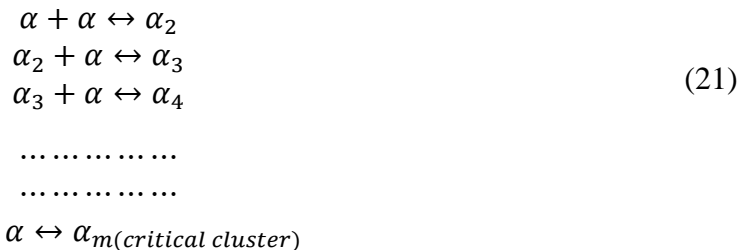
where α is a single kinetic unit and the later subscripts indicate the number of units in the cluster. Single kinetic units in the solution comes together and forms clusters. These clusters are often broken into old units. Some embryos reach critical thermodynamic energy. This critical cluster is called as nucleus and the crystallization process begins.

$$Cluster \leftrightarrow embryo \leftrightarrow nucleus \leftrightarrow crystal$$

Nuclei are in a state of unstable equilibrium: if a nucleus loses units, it dissolves; if it gains units, it grows and could become a crystal. The Gibbs free energy change of the nucleus is shown in Figure 2.6. As the cluster becomes larger than critical size, the free energy of the system decreases and the process becomes nucleation. The mechanism is the same in primary

15

homogenous and primary heterogenous nucleations. In the case of primary heterogenous nucleation, nucleation is carried out on favorable sites as energy in foreign solid impurities. The both mechanisms depend on supersaturation. Nucleation takes place quickly when supersaturation reaches critical level (Tavare, 1995; Rashid, 2011). Nucleation scheme is given in Figure 2.7. The critical free energy change is calculated as follows:

$$\Delta G_{crit} = \frac{4}{3}\pi\gamma(r_C)^2 \tag{22}$$

where r_C denotes the critical size and γ is the interfacial tension.
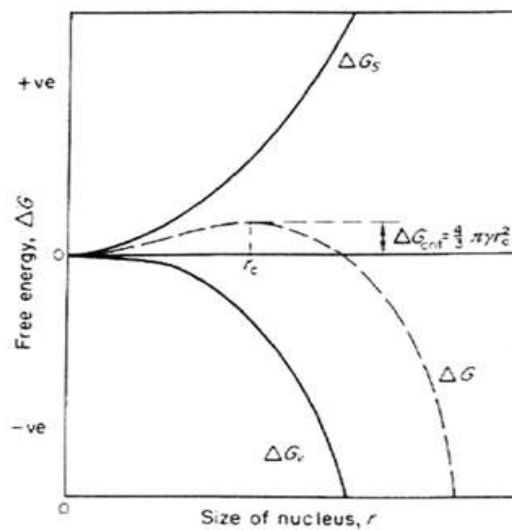
Figure 2.6. Free energy diagram for nucleation and the existence of a 'critical nucleus' (Mullin, 2001; Rashid, 2011).
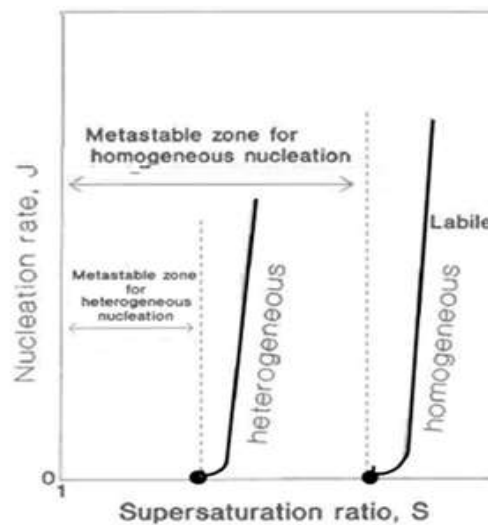
Figure 2.7. Nucleation rate and supersaturation ratio (Tavare, 1995; Rashid, 2011).

16

Secondary nucleation is the induction of the nucleation process with an external effect in the presence of crystal seeds at lower levels of supersaturation. When the nucleation kinetics is examined, it is necessary to differentiate between primary and secondary nucleation kinetics. The primary nucleation kinetics is mathematically expressed in terms of $B = dN/dt$, the change in the number of crystals per unit volume. Correlation is expressed empirically as

$$B = \frac{dN}{dt} = k_{BP}s^n \tag{23}$$

where N is the total number of crystals per unit of crystallizer, t is time, k_{BP} is a nucleation rate constant, and n is the nucleation order. The rate of nucleation is denoted as B.

Secondary nucleation kinetics is however expressed by following empricial correlation

$$B = \frac{dN}{dt} = k_B M_c^j s^n \tag{24}$$

where k_B is a nucleation rate constant, M_c is the crystal content, j is the crystal content exponent and n is the nucleation order on supersaturation. Details can be found in Rashid (2011).

2.1.7. Crystal Growth

The transformation of stable nuclei into visible crystals is defined as crystal growth. Many mechanisms and theories such as surface energy, adsorption layer, kinematic and diffusion-reaction theories have been proposed for crystal growth (Mullin, 2001).

The accumulation of mass during crystallization is given by following equation (Carbone and Etzel, 2006).

$$\frac{dM}{dt} = kA \left(\frac{c_i - c_s}{c_s}\right)^g \tag{25}$$

M is the total mass of crystal, k is the mass deposition rate constant, A is the total crystal surface area. c_i denotes the concentration adjacent to the surface of growing crystal. c_s represents the solubility. g is the growth order.

In well stirred systems c_i becomes equal to concentration in the bulk solution. Linear growth rate is defined as (Saikumar, Glatz & Larson, 1998).

$$G = \frac{dL}{dt} = k_g \left(\frac{c - c_s}{c_s}\right)^g \qquad (26)$$

G is the growth rate. k_g is the growth rate constant. c represents the concentration of the solute in solution. c_s is the equilibrium solubility. L and t are the characteristic lengt of the crystals and time, respectively.

The above formula is a generic equation that refers to the crystal growth driving force. Crystal growth is directly proportional to the characteristic size of the selected crystals. Crystal growth measurement is generally performed by batch processes. Solute concentration and amount of crystals vary depending on time. If the nucleation occurs the number of crystals varies. Two methods are used to measure the crystal growth rate. First, the single crystal method examines the time-dependent development of single crystal at certain temperature and in certain supersaturation. In the bulk method, crystals growth from solution is performed generally by one of the following crystallization methods; the isothermal crystallization, cooling crystallization, crystallization by solvent removal and anti-solvent crystallization. In isothermal crystallization, seed crystals are added into the metastable solution and the concentration in the solution decreases. Crystal growth kinetic parameters are determined by the analysis of size distributions of seeds and crystals and concentration of the solute in the bulk solution with respect to time (Rashid, 2011).

2.1.8. Crystallization Growth Kinetics of Rebaudioside A

There are limited number of studies on the solubility and crystallization of stevioside and Rebaudioside A in the literature. Solubilities of steviol glycosides in water were reported by Kinghorn (2002). The solubilities of Stevioside, Rebaudioside A, Rebaudioside B, Rebaudioside C, Rebaudioside D, Rebaudioside D, Rebaudioside E, Steviolbioside and Dulcoside A in water were reported to be 0.13, 0.80, 0.10, 0.21, 1.00, 1.70, 0.03 and 0.58 % respectively. Abou-Arab et al. (2010) extracted steviol glycosides from *Stevia rebaudiana* Bertoni with water, methanol and water-methanol mixtures and characterized the physical and chemical properties of the extracts. They obtained stevioside percentages in water, methanol and methanol mixtures as 15.82%, 23.20 and 18.62%, respectively. They examined the solubility of stevia sweeteners in water, methanol, hexane, acetone, chloroform and ether. According to their findings, stevia sweeteners were found to have high solubility in methanol. The resulting sweeteners were dissolved in water at a lower rate than that in methanol and

solubility of the sweetener was found to be 9.8%. While sweeteners were slightly soluble in hexane, they were not dissolved in acetone, chloroform and ether. Abou-Arab et al. (2010) only studied the solubility of extracted sweeteners and their study was intended to determine in which solvents the extract was soluble, rather than the observing of a thermodynamic solubility. Celaya, Kolb, and Kolb (2016) studied the solubility of Reb A in water, ethanol and water-ethanol mixtures. They found 5.0, 3.7, 3.2, 3.8, 3.8 and 6.6 g/mL solubility in water at 5, 30, 35, 40, 45, 50°C, temperatures respectively.

The literature on the crystallization of Rebaudioside A is scarce, an article written in Chinese reports the measurement of the solubility, supersaturation and metastable zone width by cooling crystallization of Reb A in methanol aqueous solutions (Zhao, Gu, Cheng, Lı & Hong, 2012). Crystallization of polymorphs of Rebaudioside A from crude solution containing 80 % Reb A were reported by Prakash, DuBois, King, and Upreti (2007). When the water content of alcohol solution is low, the solvate form crystalizes in the solution. Alcohol solutions with high water content resultsin the crystallization of hydrate form. Solvate form is converted into anhydrous form upon drying under nitrogen. Amorphous Reb A can be produced by ball milling, precipitation, spray drying, lyophilization and cryo-grinding (Prakash et al., 2007). Upreti et al. (2012) reported the growth of novel anhydrous crystal Reb A phase by the slow evaporation of Reb A solution in methanol. Three different crystal forms of Reb A (hydrated, solvated and anhydrous were also characterized in terms of X-ray indexing and unit cell parameters.

3. MATERIALS AND METHODS

3.1 Materials

The materials used in this study are given in Table 3.1. Ultrapure water (18.2 MΩ/cm) was used throughout this study.

Table 3.1. The materials used in this study.

Material	Brand	Purity
Rebaudioside A	Almendra	99.5%
Absolute Ethanol	Merck	98%
Acetonitrile	Merck	99.9%
Acetone	Merck	99%
Silica beads	Birpa	-
Silica particles (Silica gel 60)	Merck	-
Syringe mounted filter	Membrane Solutions	Nylon, 0.22 μm

3.2. Methods

3.2.1. Determination of Solubility

Water-solubilities of Reb A powder at 4, 20, 37, 40, 50 and 60 °C were determined. Excessive amount of Reb A powder was added into plastic/glass tubes containing 10 mL of deionized water which was previously heated to the temperature where the solubility would be measured. Triplicate samples were prepared for the determination of the solubility at each temperature. Tubes were tightly closed and incubated for 2 weeks at above stated temperatures. Certain amount of supernatant was taken by 5 mL capacity polypropylene syringe and then filtered through in 0.22 μm Nylon filter. Filtered supernatant was taken into volumetric flasks containing deionized water whose weight was previously recorded and weighed. After diluting to 100 mL using deionized water and mixing thoroughly, Reb A concentration was determined.

Solubility values of Reb A seed prepared from crystals grown in water at 60 °C were also determined at 20, 30, 40, 50 and 60 °C in a similar way reported above.

3.2.2. Preparation of Crystalization Seeds

Crystal seeds were prepared for use in the secondary nucleation threshold determinations. Different methodologies were used to prepare proper crystal seeds.

3.2.2.1. Seed Crystals Prepared in a Rotary Evaporator

Ultra-pure water, ethanol, or water-ethanol mixtures were used as solvents in the preparation of seeds. Excessive amount of Reb A was added into the solvent. Solution was mixed thoroughly. They were centrifuged for 5 minutes at 7000 rpm. The supernatant was taken and filtered through 0.22 μm Nylon filters to give saturated Reb A solution. Reb A was then recrystallized from the saturated solution in a rotary evaporator under vacuum. All powders were gently ground in an agate mortar. The solvents, solid/liquid ratio and crystallization temperatures are shown in Table 3.2.

Table 3.2. Seed crystals prepared in rotary evaporator.

Sample	Solvent	Solid/Liquid Ratio	Temperature (°C)	Rotary Evaporator (RPM)
S1	Ultrapure water	7.5276 gr/20 mL	80	200
S2	96% ETOH	1.080 gr/20 mL	30	200
S3	Ultrapure water	6.07 gr/20 mL	80	200
S4	Ultrapure water	8.1576 gr/20 mL	30	200
S5	Abs. ETOH	1.0155 gr/20 mL	50	-
S6	Ultrapure water	7.5273 gr/20 mL	80	200
S7	Ultrapure water	6.07 gr/20 mL (without grinding in agate mortar)	80	200
S8	Abs. ETOH	1.0792 gr/20 mL	30	200
S9	96% ETOH	1.0836 gr/20 mL	50	-
S10	80% ETOH	2.0127 gr/20 mL	50	200
S11	Ultrapure water	6.8309 gr/20 mL	50	200

3.2.2.2. Seed Crystals Prepared from Saturated Reb A Solution by Water Removal

Reb A saturated ethanol-water mixtures were prepared by mixing excessive amount of Reb A powder with ethanol-water mixtures and filtering through 0.22 μm Nylon filter. Silica beads or silica powder wrapped in a filter paper was added into the tubes to allow the adsorption of water in order to grow crystals due to the differences in solubility. The specifications of the experiments are shown in Table 3.3.

Table 3.3. Seed crystals prepared by removal of water using silica beads or silica particles from saturated Reb A solutions.

Sample	Solvent	Additional applications	Silica particles & Silica beads
S12	90% ETOH	filtration through filter paper	Silica particles
S13	90% ETOH	4000 rpm 2 minute + 6000 rpm 5 minute centrifuge	Silica beads
S14	90% ETOH	Vortex mixing	Silica beads
S15	90% ETOH	0.22 μm syringe filter filtration	Silica particles
S16	80% ETOH	-	Silica beads
S17	80% ETOH	0.22 μm syringe filter filtration	Silica particles
S18	96% ETOH	0.22 μm syringe filter filtration	Silica particles

3.2.2.3. Seed Crystals Prepared by Precipitation

Saturated Reb A solutions prepared in ultrapure water were added dropwise into acetone or acetone was added dropwise into the solutions while stirring. Table 3.4 shows the sample codes and the addition rate of solution/acetone.

Table 3.4. Seed crystals prepared in acetone.

Sample	Addition Rate	Methods of Addition
S19	-	Acetone addition into Reb A solution
S20	5 min.	Acetone addition into Reb A solution
S21	17 min. 58 sec.	Acetone addition into Reb A solution
S22	Sudden addition	Reb A solution addition into acetone
S23	-	Reb A solution addition into acetone

3.2.2.4. Seed Crystals Obtained by Dry Milling

Reb A powder was dry milled either by using hand-shaking the Reb A powder and zirconia balls in a polypropylene bottle or by grinding using IKA (A11 Analytical Mill, Germany) grinding mill (Table 3.5). Sample milled using zirconia balls were also further subjected to grinding in an agate mortar for 20 minutes. Samples were taken at 5 minutes intervals during grinding.

Table 3.5. Seed crystals obtained by dry grinding.

Sample	Grinding Apparatus	Grinding Time (min)
S24	Zirconia balls	30
S25	IKA grinding mill	5

3.2.2.5. Seed Crystals Obtained by Centrifugal Milling

Seed crystals were prepared by milling Reb A powder in a centrifugal mill (Retsch ZM 200). Two different types of seeds (S26 and S27) were prepared by milling. A sample, S26, was prepared by milling the powder at 10000 rpm. Another sample (S27) was prepared by milling the powder sequentially 5 times at 10000 rpm.

3.2.2.6. Seed Crystals Prepared by Crystallization at Constant Temperature

Six grams of Reb A was dissolved in 40 mL of deionized water by shaking thoroughly. The solution was placed in a laboratory oven at 60 °C. Crystals were separated from the solution by centrifugation for 15 minutes at 9000 rpm after 24 hours and dried in a vacuum oven at 60 °C. The crystals were finally ground in the centrifuged mill at 6000 rpm. This sample was denoted as A1.

3.2.3. Determination of Nucleation Thresholds

Primary and secondary nucleation tresholds of Reb A powder in water were determined isothermally in two different systems, static and stirred double-jacketed reactor.

3.2.3.1. Primary Nucleation Tresholds

Primary nucletion threshold determinations were performed both in a static system by holding Reb A solutions at constant temperature in a water bath and in a stirred double-jacketed reactor. A home-made crystallization apparatus consisted of a two-liter jacketed vessel connected to a circulating water bath and an overhead stirrer shown in Figure 3.1 was used in the determination of primary nucleation tresholds of Reb A in water under stirring at 300 rpm.

Figure 3.1. Crystallization apparatus.

3.2.3.1.1. Determination of Primary Nucleation Thresholds in the Static System

Primary nucleation thresholds of Reb A at 25, 40, 50 and 60 °C in the static system were determined by holding the tubes containing Reb A in different solid to liquid ratios (mass (g)/volume (mL)) in a constant temperature water bath.

Turbidities of the samples in FAU units were measured at certain time intervals at wavelength of 550 nm in Merck Pharo 300 UV-Visible spectrophotometer. Solid/liquid ratios of the solutions used in the determination of primary nucleation thresholds are given in Table 3.6.

Table 3.6. Solid/liquid ratios of samples used in the determination of primary nucleation threshold in a static system.

Mass of Reb A (g)	Volume of Water (mL)	Solid to Liquid Ratios (g/mL)
0.25	10	0.025
0.4	10	0.04
0.8	10	0.08
0.3	10	0.03
0.2	10	0.02
0.1	10	0.01
2	10	0.2
0.04	10	0.004
0.025	10	0.0025
0.01	10	0.001

3.2.3.1.2. Determination of Primary Nucleation Thresholds in the Stirred Recator

Primary nucleation tresholds of Reb A at 20, 30, 40 and 50 °C were determined in the crystallization apparatus. Two hundred fifty five mL of water was added into the vessel. Water was heated to the nucleation temperature. Certain amount of Reb A was dissolved in the water. The speed of stirrer was set to 300 rpm. Solution was then heated to the temperature 10°C above the nucleation temperature in order to dissolve ghost nuclei which could possibly be formed in the solution. The solution was then cooled to the nucleation temperature. Evaluation of nucleation was performed by visual inspection.

3.2.3.1. Secondary Nucleation Thresholds

Secondary nucleation tresholds of Reb A in water were determined both in static sytem and in the reactor by isothermal crystal growth experiments.

3.2.3.1.1. Determination of Secondary Nucleation Thresholds in the Static System

Secondary nucleation thresholds of Reb A at 20, 30 and 40 °C in the static system were determined by preparing Reb A solutions in different solid to liquid ratios (mass (g)/volume (mL)) (Table 3.7).

Table 3.7. Solid to liquid ratios used in the determination of secondary nucleation thresholds in a static system.

Mass (g)	Volume (10 mL)	Solid to Liquid Ratios (g/mL)
0.2	10	0.02
0.1	10	0.01
0.08	10	0.008
0.07	10	0.007
0.06	10	0.006
0.05	10	0.005
0.04	10	0.004
0.03	10	0.003
0.02	10	0.002
0.01	10	0.001
0.0045	10	0.00045

Reb A powder was dissolved in 10 mL water. Tubes were placed in a water bath. Temperature of the water bath was increased 10° C higher than the corresponding temperature in order dissolve possible ghosh nuclei. Temperature was then decreased to desired temperature.

Approximately 15 mg seed was added into 5 mL ultrapure pure water and dispersed by 5 minutes-sonication. 0.1 mL seed dispersion was then added into tubes and solutions were shaken. The presence of nucleation was determined visually by checking the solutions hourly within 10 hours.

3.2.3.1.2. Isothermal Crystal Growth Experiments in the Reactor

Secondary nucleation treshold determination and crystal growth experiments were performed by isothermal crystal growth experiments. Isothermal crystal growth experiments were performed for 300 rpm at 20, 30 and 40 °C. Two hundred fifty five mL of deionized water

were added into the crystallization vessel. Water was heated to the nucleation temperature. Certain amount of Reb A was the dissolved in the water. Temperature was first increased to the point which was 10 °C higher than the nucleation temperature in order to dissolve ghost nuclei. The solution was then cooled down to the nucleation temperature. One milliliters of seed dispersion prepared by 5 minutes-sonication of seed solution containing 15 mg seed (A1) in 5 mL ultrapure pure water was added into the reactor. The presence of secondary nucleation was inspected visally and by absorbance measurement. Five milliliters of samples were taken from the solution in 24 hours invervals. Samples were centrifuged for 10 min at 9000 rpm. Supernatants were then filtered through syringe mounted 0.22 μm Nylon filter. One milliliter from filtered supernatants was diluted to 25 or 50 mL with deionized water. Absorbance of the solutions were measured at 210 nm.

Table 3.8. Solid to liquid ratios used in the isothermal crystal growth experiments.

	Temperature (°C)		
	20	**30**	**40**
Solid to liquid ratio (g/mL)	0.0025 0.004 0.01	0.003 0.0035 0.0055	0.0035

3.2.4. Characterization of Rebaudioside A Crystals

Reb A starting powder, seeds prepared and crystals grown were characterized by X-ray diffraction, optical microscope and scanning electron microcope. The particle size distribution was determined by particle size analysis.

3.2.4.1. X-Ray Diffraction

Crystal structures of powders were determined by X-Ray Diffraction (XRD) analysis using Rigaku Miniflex600 X-Ray Diffractometer (Japan). XRD patterns of the samples were determined by scanning from 2θ values of 5-80 with a step size of 0.02 and scanning rate of 2θ/min.

3.2.4.2. Optical and Scanning Electron Microscopy

Morphologies of the starting power, seeds prepared and crystals grown were determined by using polarized light microscope (Olympus BX51-P, Japan) and scanning electron microcope (SEM) equipped with a secondary electron (SE) detector (Zeiss Supra 55, Germany) SEM micrographs of the samples were obtained after platinium coating of the samples.

3.2.4.3. Particle Size Measurement

Particle sizes of Reb A powders were measured by using Malvern Mastersizer 3000. Absolute ethanol was used as a dispersing medium. Ultrasonication was applied for the dispersion of powder. Refractive index values of Reb A and absolute ethanol were taken as 1.51 and 1.36 respectively.

3.2.5. Analytical Methods

Two different analytical methods (high pressure liquid chromatography and UV-Visible spectrophotometer based methods) were used for the determination of Reb A concentration in the solutions.

3.2.5.1. High Pressure Liquid Chromatography (HPLC)

High pressure liquid chromatography (HPLC) (Agilent 1260, Santa Clara, USA) equipped with a C-18 Isis column (1.8 μm, 100 mm x 4.6 mm, Nucleodur, Macherey-Nagel, Germany) and a diode array detector was used for the determination of Reb A in the solutions. Water-acetonitrile mixture (70:30, v/v) with a flow rate of 0.6 mL/min was employed as a mobile phase. Column temperature was adjusted to 40 °C. Injection volume was 20 μL. Detection was performed at the wavelength of 210 nm.

Reb A stock solution with a concentration of 1000 mg/L was prepared by dissolving 0.1 g dried powder in ultrapure water and diluting to 100 mL in a volumetric flask. Two different sets of standard solutions were prepared from the Reb A stock solution for the construction of calibration curves. One set included nine standard solutions with concentrations of 10, 20, 30, 40, 50, 60, 70, 80 and 90 mg/L whereas the other had six standard solutions at different concentrations 100, 120, 140, 160, 180 and 200 mg/L. Stock solution and all standard solutions were prepared in triplicate. Three samples were taken from each standard solution and analyzed using HPLC.

Another HPLC based method was also used for the samples in which decomposition of Reb A migh have occurred (70, 80 and 90 °C). HPLC (Agilent 1260, Santa Clara, USA) equipped with a C-18 Capcel column (5 μm, 250 mm x 4.6 mm, Phenomenex, Shiseido, Japan) was used. Water-acetonitrile mixture (70:30, v/v) with a flow rate of 1 mL/min was employed as a

mobile phase. Column temperature was adjusted to 40°C. Injection volume 5 μL was selected. Detection was performed at the wavelength of 210 nm.

3.2.5.2. UV-Visible Spectrophotometric Methods

Absorbance values of the standard solutions were measured in a quartz cuvette with 1 cm path-length using Agilent UV-Visible spectrophotometer (Cary 60, Santa Clara, USA) at 210 nm wavelength.

4. RESULTS AND DISCUSSION

4.1. Solubility of Rebaudioside A in Water

Solubilities of Reb A in water at 40, 50 and 60 °C were determined in this study. Solubilities at 4, 25 and 37 °C were previously determined by our research group (Cetin et al. (2015)). These solubility values are tabulated in Table 4.1. Solubility at 4 °C was found to be 3.7 mg Reb A/g water. When temperature was increased to 25 °C, the solubility of Reb A decreased to 2.9 mg Reb A/g water. Increase in the temperature to 37 °C however resulted in the increase of solubility to 3.7 mg Reb A/g water. Solubility of Reb A was found to increase with further increase in the temperature. Solubility values at 40, 50 and 60 °C were measured as 3.94, 5.93 and 10.65 mg Reb A/g water, respectively. Studies on the solubility of Reb A are limited in the scientific literature. Kinghorn (2002) reported the solubility of Reb A in water as 0.8 %. Although thermodynamic solubility of Reb A at 25 °C is reported to be 0.8 g Reb A/100 g water, amorphous, anhydrous and solvate forms of Reb A gives supersaturated solutions in water (>20 g/100 g at 25 °C) (Prakash et al., 2008). Reb A recrystallizes as hydrate form supersaturated solutions obtained by dissolving amorphous, anhydrous and alcohol solvate forms in water (Prakash et al., 2008). This hydrate form exhibits lower dissolution in water (< 0.2 g/100 g at 25°C) (Prakash et al., 2008). Recently solubilities of Reb A in water, ethanol and water-ethanol mixures at various temperatures were reported by Celaya et al. (2016). Solubilities of Reb A in water at 5, 30, 35, 40, 45 and 50 °C were reported to be 5.0, 3.7, 3.2, 3.8, 3.8, and 6.6 mg/L. Solubilities at various temperatures except that at 4 °C and the temperature dependent solubility behavior of Reb A found in our study were similar to those reported by Celaya et al. (2016). Calibration curves used in all concentration determinations can be found in Appendıx A1.

**Table 4.1.** Temperature dependent solubility of Reb A powder in water.

Temperature (°C)	Solubility (mg Reb A/g water)
4	3.70*
25	2.90*
37	3.70*
40	3.94
50	5.93
60	10.65

* Cetin et al. (2015).

Solubilites of Reb A in water at 70, 80 and 90 °C were also determined in this study. Clear light-yellow colored solutions were obtained after incubation at 80 and 90 °C. HPLC analysis used to determine steviol glycoside composition of stevia leaves was employed in order to check whether the decomposition had occurred or not. HPLC chromatogram of 100 and 400 mg/L Reb A solution is given in Figure 4.1.
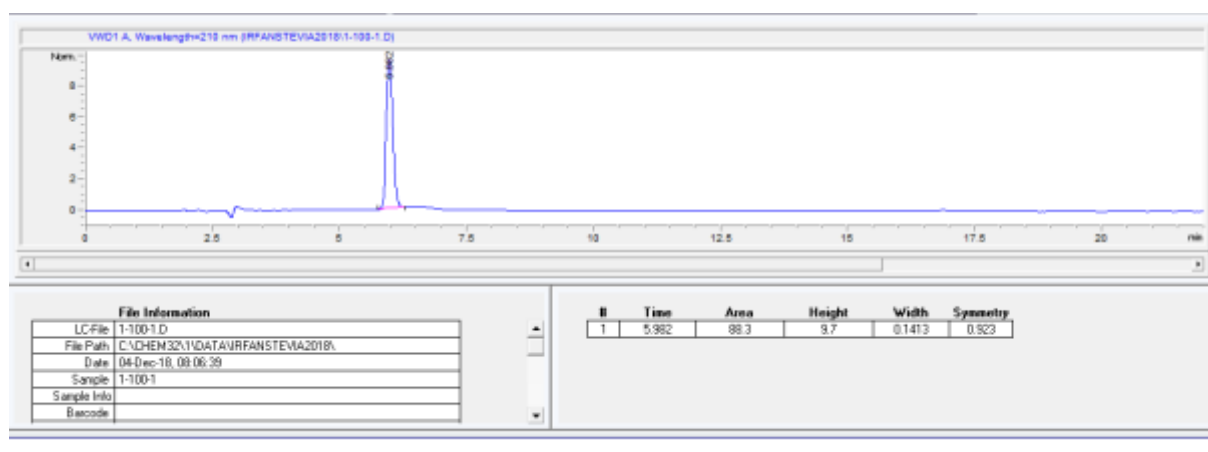

(a)
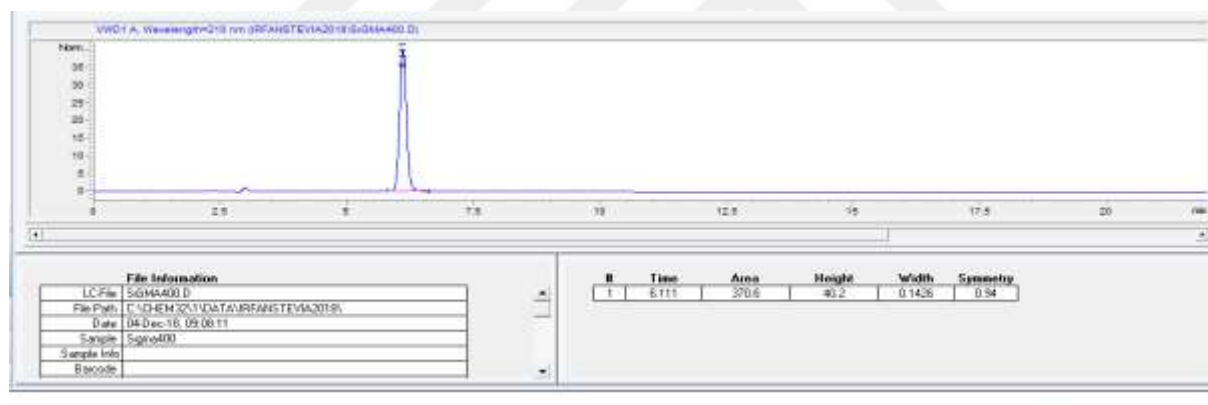
(b)

Figure 4.1. HPLC chromatograms of Reb A standard solutions (a) 100 mg/L and (b) 400 mg/L.

HPLC chromatogram of the solutions prepared by diluting samples incubated for 2 week at 80 °C with water is given in Figures 4.2 for comparison. A new peak at 17.5 min which did not observed in the HPLC chromatograms of standard solutions was detected in this chromatogram. Sample from Reb A solution used to determine solubility at 90 °C was taken at the end of 2nd day of incubation and diluted with water. The presence of the new peak was obvious in the HPLC chromatogram of this solution (Figure 4.3).

30
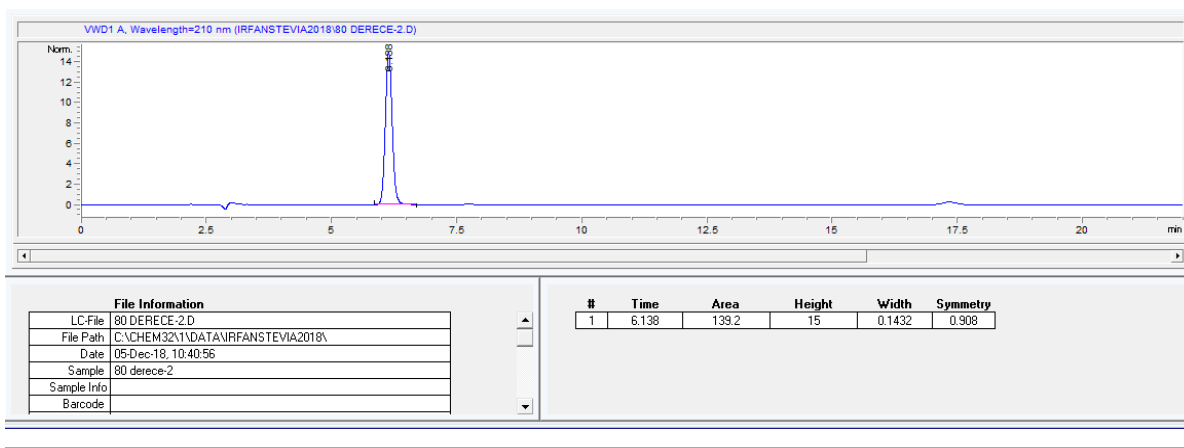
Figure 4.2. HPLC chromatogram of sample prepared by diluting Reb A solution incubated at 80 °C.
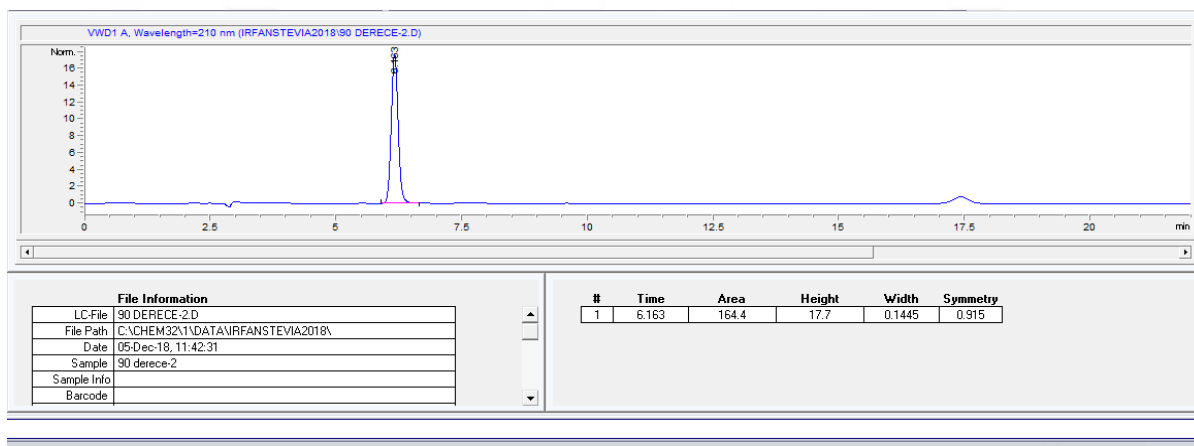
Figure 4.3. HPLC chromatogram of sample prepared by diluting Reb A solution incubated at 90 °C .

Solutions used to measure Reb A concentration in the solutions diluted from solubility samples taken from 40, 50, 60 and 70 °C were also analyzed by this HPLC methods in order to check the presence of the peak at around 17.5 min. The chromatograms are given in Appendix A.2. This peak was also detected in the chromatograms of the samples prepared by diluting solubility sample obtained at 70 °C. Solubilitiy values at 40, 50 and 60 °C are therefore given in this thesis.

The degredation of Reb A in acidic medium has been reported in the literature (Prakash, Clos & Chaturvedula, 2012). pH of deionized water is slightly acidic due to the solubility of CO_2. Since the Reb A solutions prepared in deionized water were incubated at higher temperatures, the degredation rate of Reb A might have been increased.

Gel-like precipitates in Reb A solutions prepared for the determination of solubility values were observed at the end of 2 weeks. Clear solutions distinctively separated from the precipitates were observed in the solutions. The volume of the precipitates was higher than the volume of the excessive powder initially present in the solutions. Complete gelation entrapping all the liquid phase was also occurred in several cases. Optical microscopy was therefore used to determine the morphology of precipitates. Figure 4.4 shows the optical microscope images of the starting Reb A powder. Starting powder consisted of short rod-like crystals and relatively bigger rounded crystals. Detailed particle morphology of the Reb A powder was also determined by scanning electron microscopy (Figure 4.5). Scanning electron micrograph showed that Reb A had crystals in varying length and thickness. The length of the particles, in general, was greater than 4 μm.
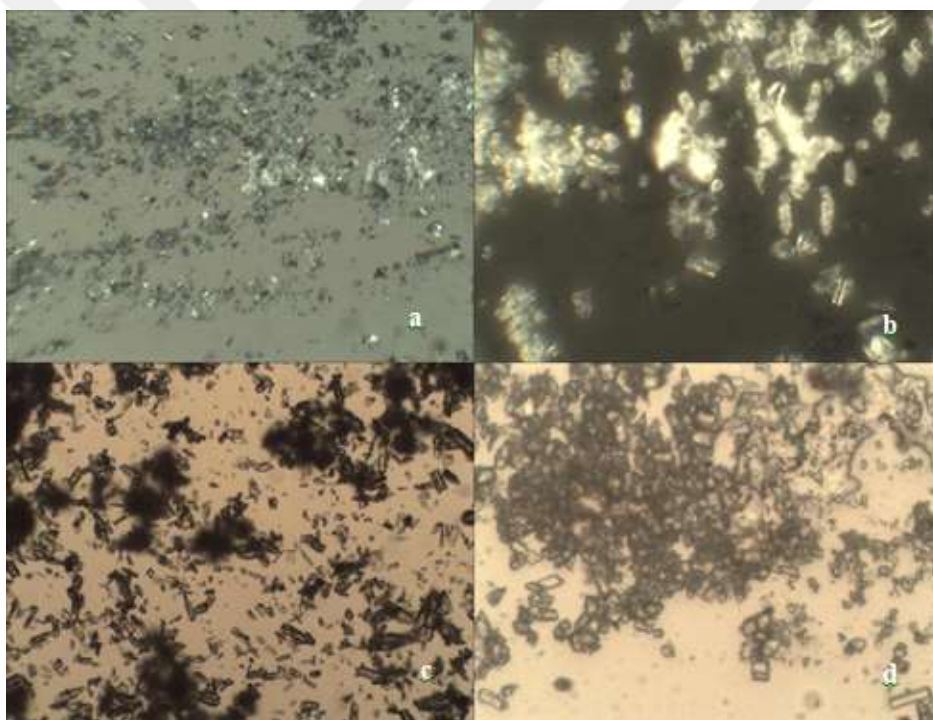
Figure 4.4. Optical microscopy images of starting Reb A powder, (a) 200X magnification, (b) 500X magnification, (c) 100X magnification, (d) 400X magnification.
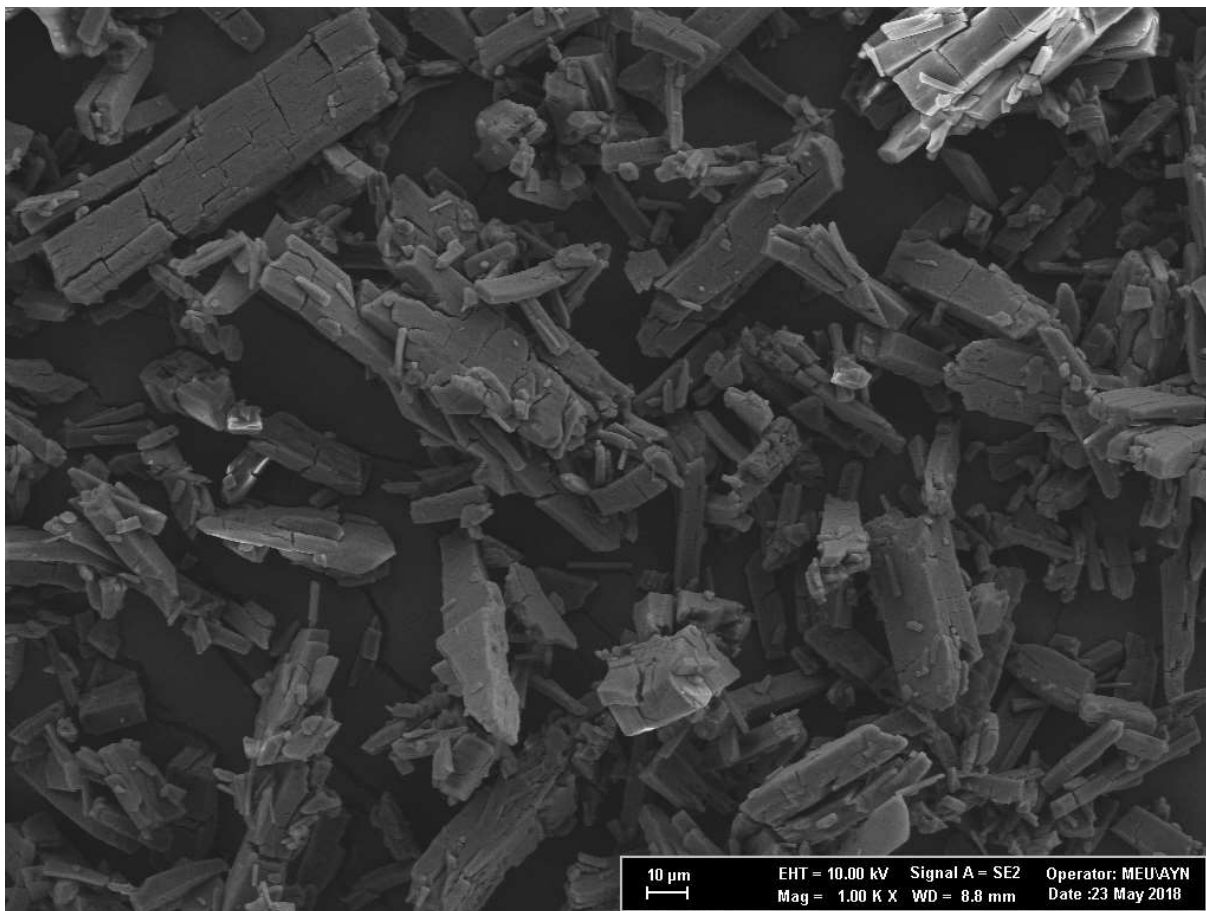
Figure 4.5. SEM image of Rebudioside A.

Particle size distribution of Reb A starting powder was measured by Malvern Master Sizer. As it is inferred from Figure 4.6, original Reb A powder contained particles smaller than 45.6 μm. Volume based median particle size of the powder was found to be 15 μm.
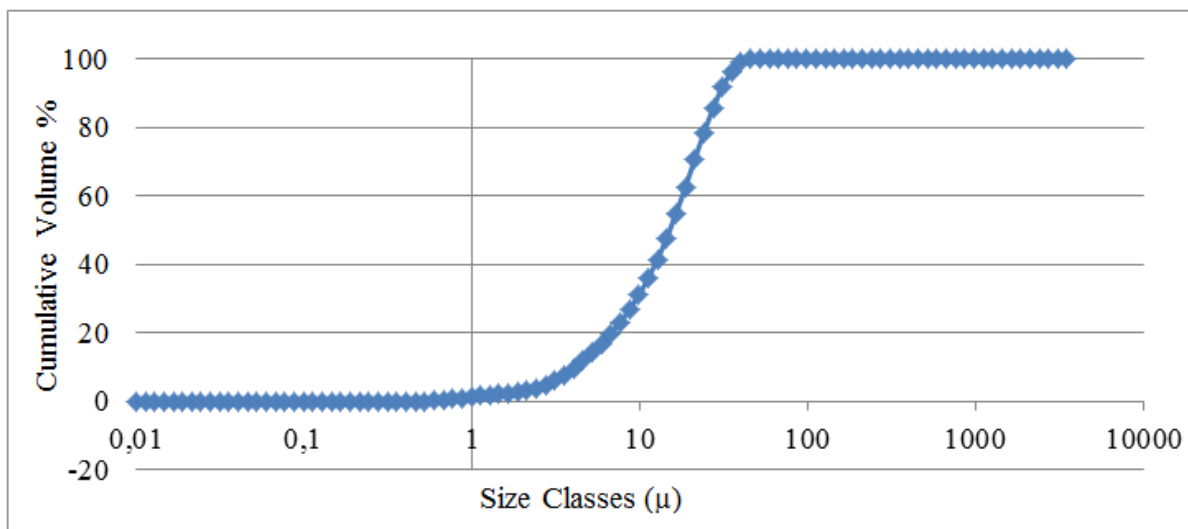

Figure 4.6. Measurement of particle size distribution of Reb A starting powder.

Optical images of Reb A crytals grown during solubility determinations at 40, 50 and 60 °C are shown in Figures 4.7, 4.8, and Figue 4.9, respectively. Optical images of Reb A crystals grown in water showed that Reb A powder recrystallizes as thin and long, whisher-like crystals from supersaturated solution in water. Gel-like appearence of the precipitates were related to the packing of particles due to the gravity. The packing of the thin and long crystals possible generates higher volume of voids in the precipiates and the water is entrapped in these voids generating gel-like appearance.
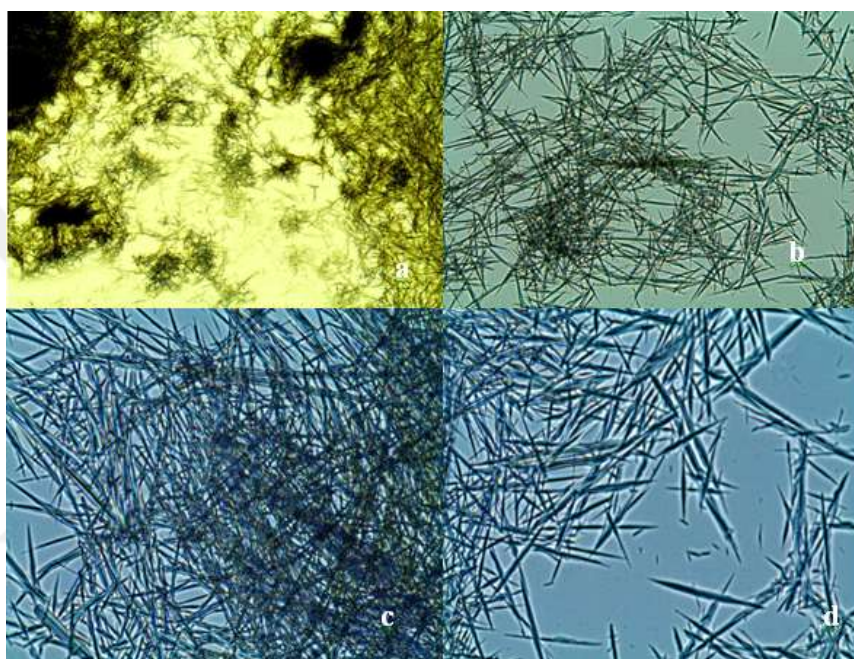
Figure 4.7. Morphology of the crystals grown at 40 °C (a) 40X (b) 200X (c) and (d) 400X magnifications.

Various methods were used to prepare Reb A seeds to be used in the determination of secondary nucleation tresholds and crystal growth of Reb A in water. One method employed was to prepare Reb A crystals from supersaturated solution at 60 °C. This seed was ground to obtain a seed which had crystal structure of water grown Reb A crystals. Solubility of this seed was also determined in this study. Solubility values of Reb A seed at 20, 30, 40, 50 and 60 °C are given in Table 4.2. Solubility of the Reb A seed was found to be lower than the solubility of the Reb A starting powder in water. Temperature dependent solubility values of starting Reb A powder and seed prepared are given in Figure 4.10.
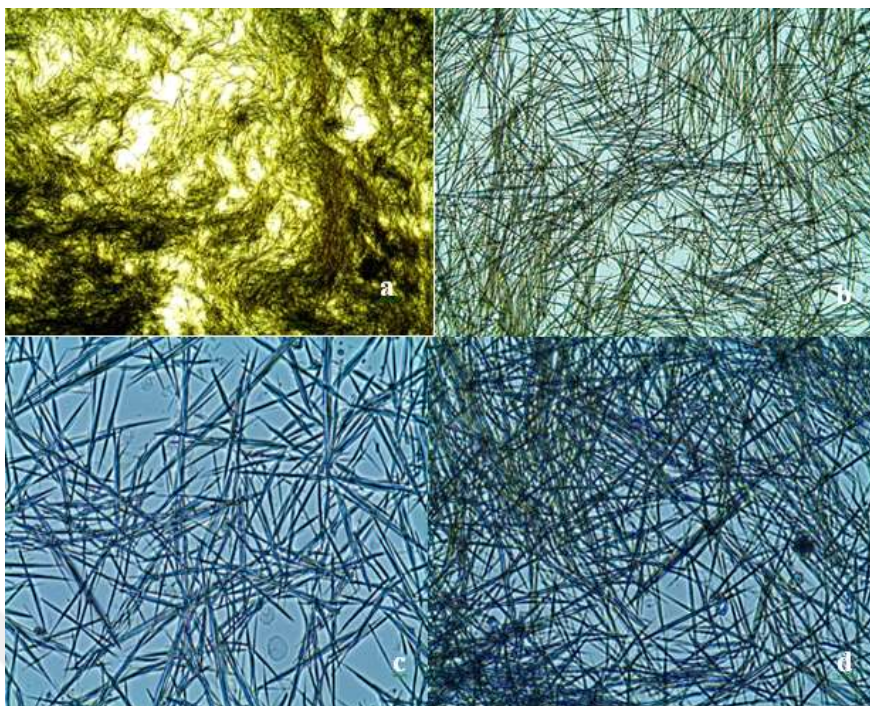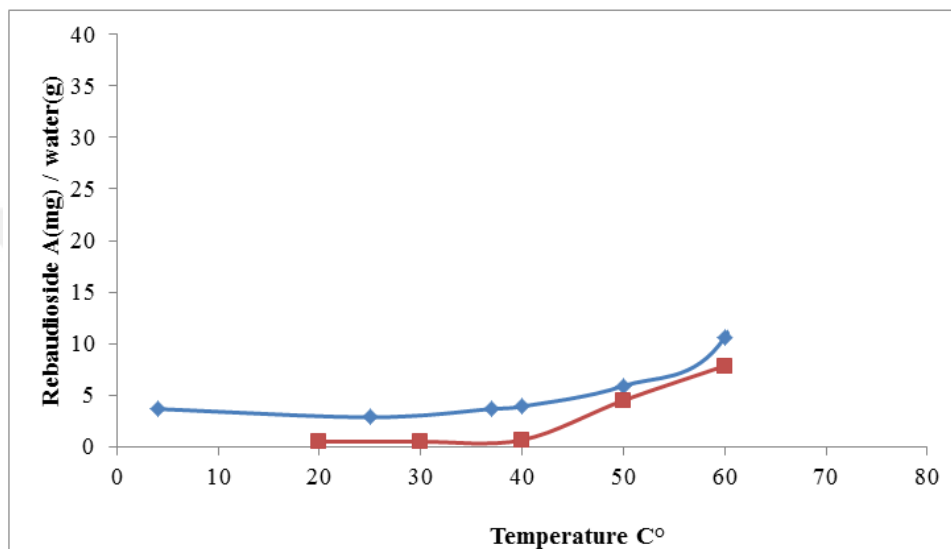
Figure 4.8. Morphology of the crystals grown at 50 °C (a) 40X (b) 200X (c) and (d) 400X magnifications.
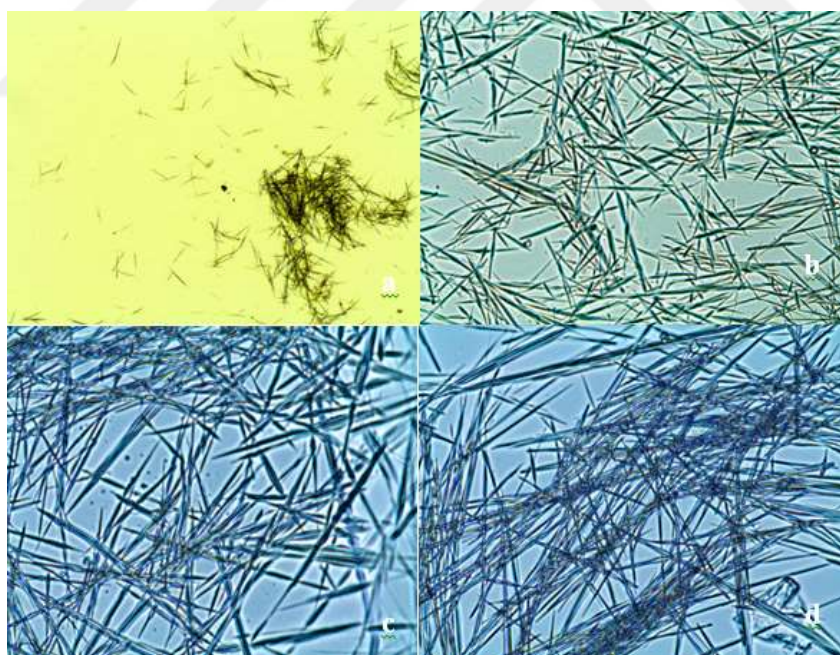
Figure 4.9. Morphology of the crystals grown at 60 °C (a) 40X (b) 200X (c) and (d) 400X magnifications.

Table 4.2. Temperature dependent solubility of Reb A seed (A1).

Temperature (°C)	Solubility (mg Reb A/g water)
20	0.55
30	0.52
40	0.70
50	4.53
60	7.87

Figure 4.10. Temperature dependent solubility values of starting Reb A powder and Reb A seed (A1).

4.2. Preparation of Seeds

4.2.1. Seed Crystals Prepared by Solvent Removal in Rotary Evaporator

Optical microscopy images of seed crystals prepared at 80°C in ultrapure water (S1, S3, S6 and S7) are given in in Figures 4.11, 4.12, 4.13, and 4.14, respectively.
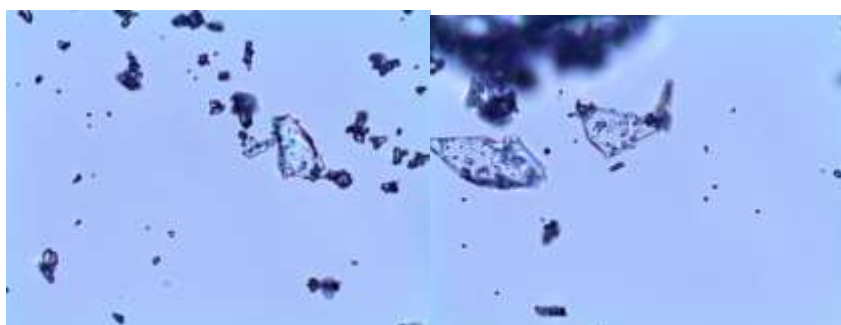
Figure 4.11. Optical microscopy images of S1 (400X).

Particle size distribution of the samples crystallized at 80 ºC was very wide. The film formation was also observed during the seed preparation in the rotary evaporator. Although the crystallized seeds were ground by agatate mortar, the presence of larger transparent particles were evident in optical micrographs.

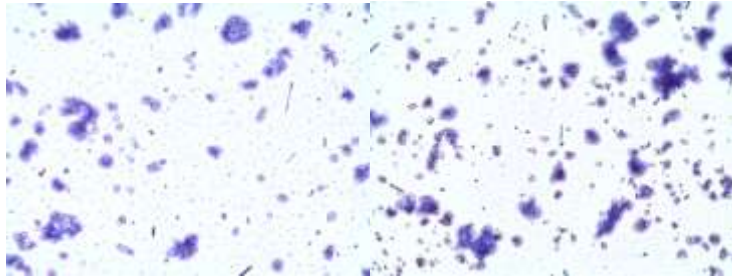**Figure 4.12.** Optical microscopy images of S3 (400X).
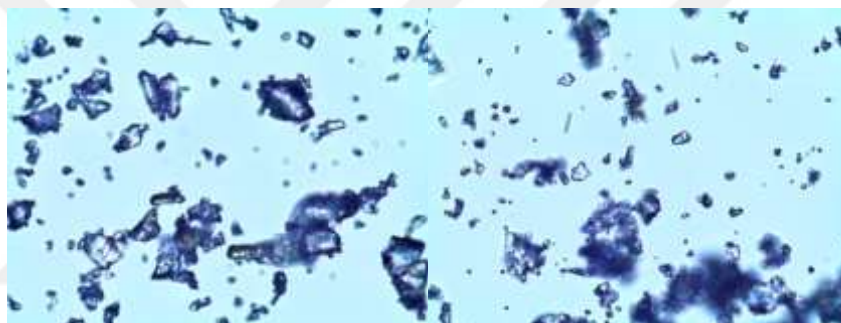
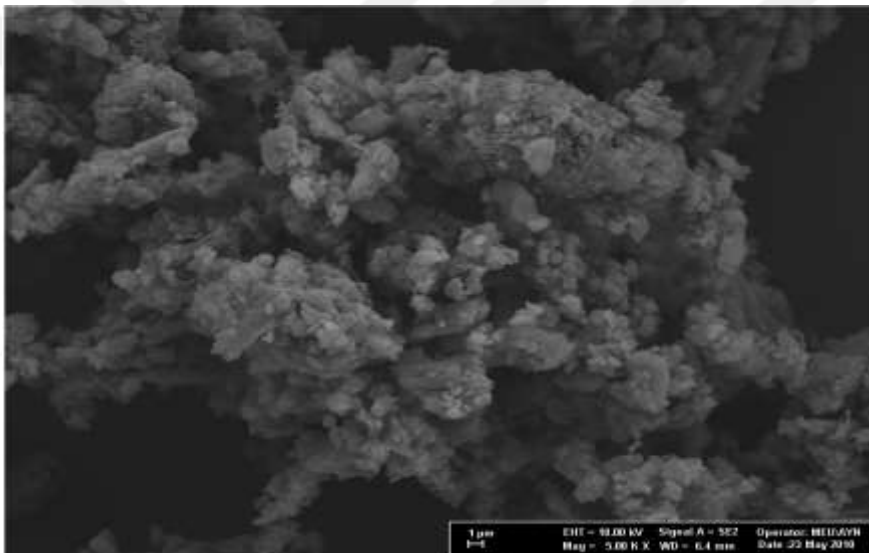**Figure 4.13.** Optical microscopy images of S6 (400X).
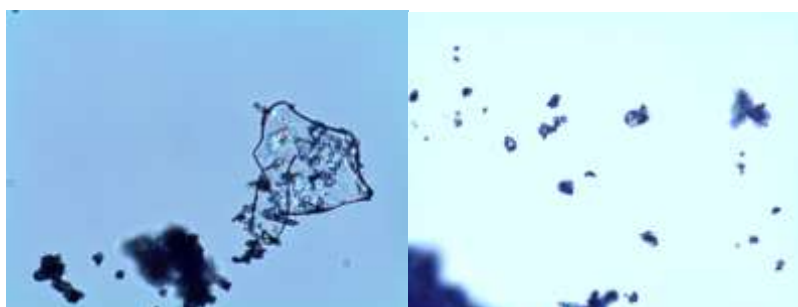
Figure 4.14. Optical microscopy images of S7 (400X).

The particle sizes of the sample prepared in water at 50 ºC (S11) was found to be small but the particle size distribution was large (Figure 4.15).

Figure 4.15. Optical microscopy images of S11 (400X).

Detailed determination of the particle size and morphology of Sample S11 using scanning electron microscopy showed that powder contained agglomerated small and large particles (Figure 4.16).

Figure 4.16. SEM image of S11.

Sample prepared at 30 ºC (S4) was observed to have a wide particle size distribution (Figure 4.17).

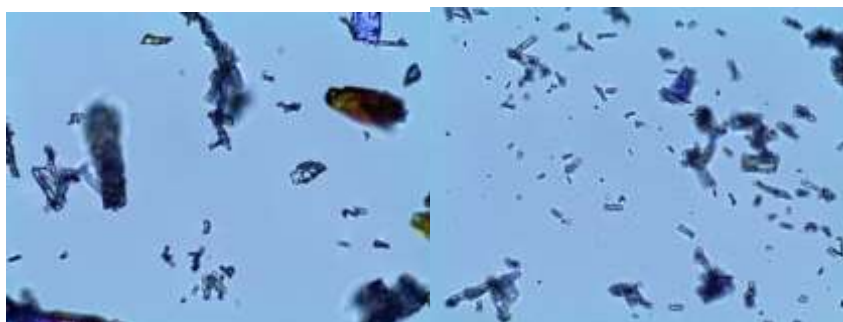**Figure 4.17.** Optical microscopy images of S4 (400X).

An optical microscope image of the sample obtained by crystallization in absolute ethanol at 80 ºC in the rotary evaporator is given in Figure 4.18. As it is inferred from Figure 4.18, the Reb A crystals were composed of elongated crystals and wide plates. Figure 4.19 and Figure 4.20 show microscope images of the crystallized powder at 50 ºC and 30 ºC, respectively in the rotary evaporator from saturated Reb A solution prepared in absolute ethanol. It was observed that Reb A films formed at both temperatures and these film layers were ground into plates in varying size.

Figure 4.18. Optical microscopy images of S28 (400X).
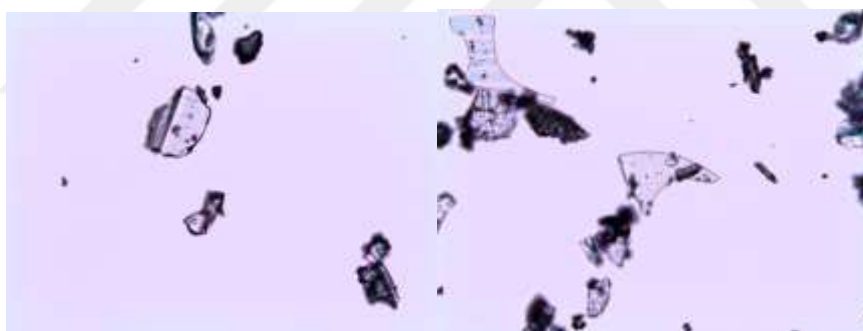
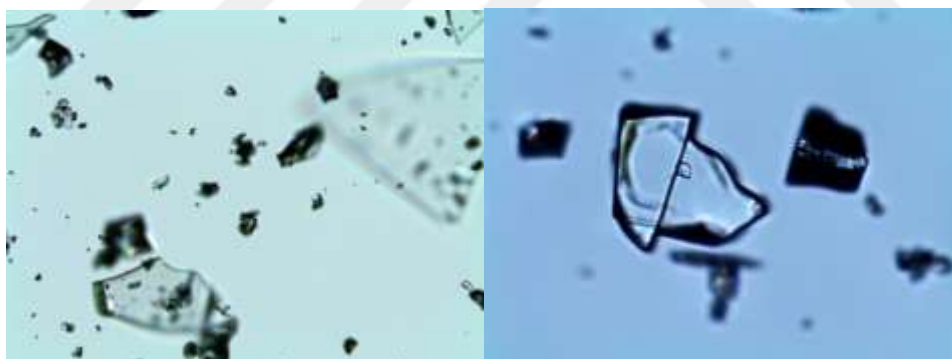**Figure 4.19.** Optical microscopy images of S5 (200X).

Figure 4.20. Optical microscopy images of S8 (400X).

Due to the inability of obtaining suitable crystals at different temperatures in pure water and absolute ethanol, ethanol water mixtures were prepared. Saturated Reb A solutions were prepared in these mixtures and crystals were obtained by evaporation of the solvent in the rotary evaporator. Microscopic images of the crystal seeds prepared at 50 ºC and 30 ºC from saturated solutions prepared in 96 % (v/v) ethanol are shown in Figure 4.21 and Figure 4.22, respectively. The crystals prepared at 50 ºC were composed of agglomerated rounded particles while coarse transparent plates were obtained at 30 ºC.

Figure 4.21. Optical microscopy images of S9 (400X).

Figure 4.22. Optical microscopy images of S2 (a) 200X and (b) 400X.

The morphology of the crystals obtained in the rotary evaporator from the saturated Reb A solution prepared in 80 (v/v) % ethanol at 50 ºC showed the presence of both small particles and large film-ground plates (Figure 4.23).

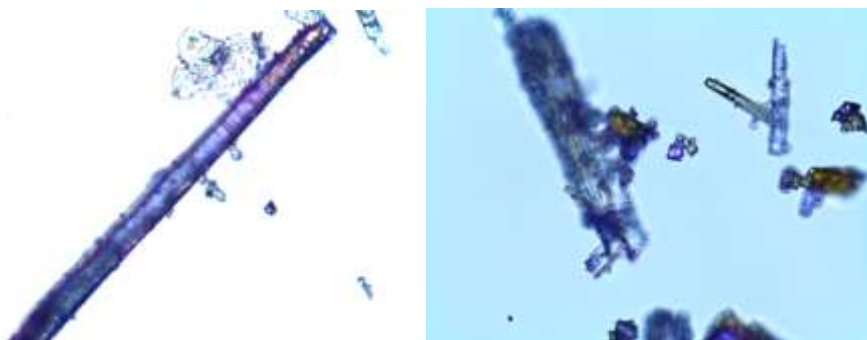**Figure 4.23.** Optical microscopy images of S10 (400X).

Analysis of the particle morphology by SEM showed that nearly rounded small particles coexisted with large plates (Figure 4.24). These plates are possibly the large transparent particles observed by optical microscope.
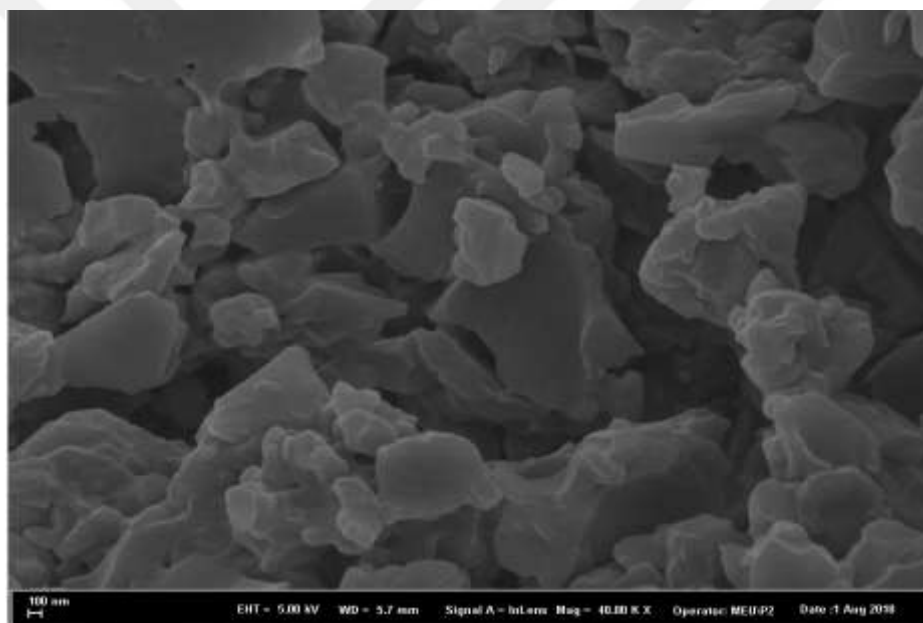
Figure 4.24. SEM image of S10.

4.2.2. Seed Crystals Prepared from Saturated Reb A Solutions by Water Removal

The optical micrographs of the S18, produced by adding 2 grams of silica particles in 96% ethanol as an adsorbent for water removal is shown in Figure 4.25. The crystals formed by this method were observed to be long but thin and thick rods.
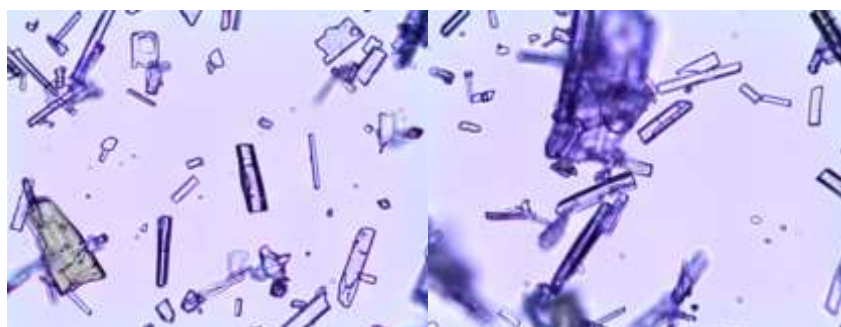
Figure 4.25. Optical microscopy images of S18 (a) 200X and (b) 400X.

The sample, S12 was obtained by controlled crystallization by adsorption of water from saturated Reb A solution prepared in 90% ethanol by the addition of 10 g silica. The seed crystals formed by this method formed long, thick and large crystals (Figure 4.26).
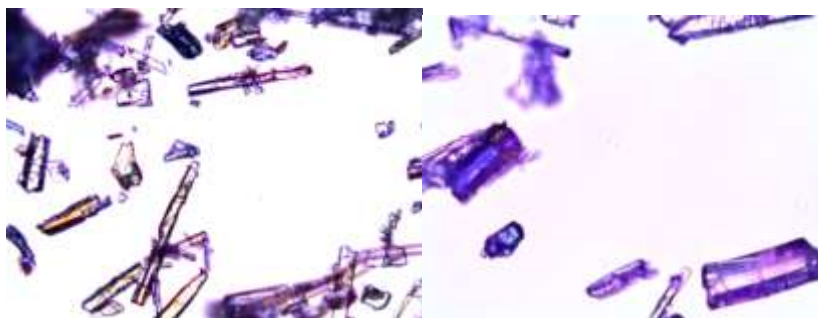

Figure 4.26. Optical microscopy images of S12 (400X).

Samples S13 and S14 were prepared by using silica beads as water adsorbing agent in Reb A saturated solutions prepared in 90 % ethanol. The resulting crystals were observed as plates of different sizes and elongated rods (Figure 4.27 and Figure 4.28 for Sample S13 and Sample S14, respectively).
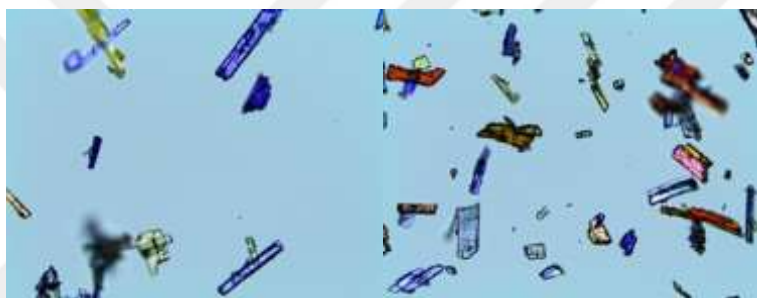

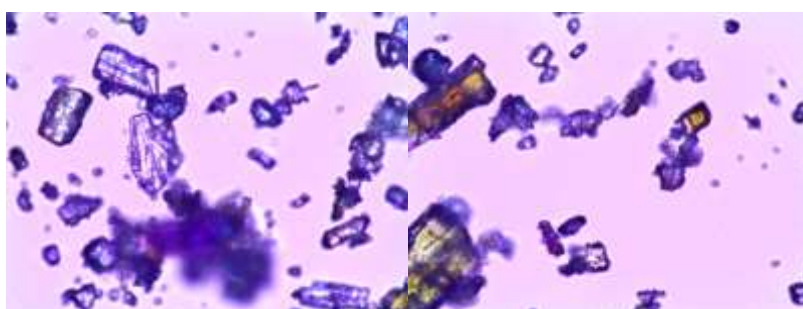**Figure 4.27.** Optical microscopy images of S13 (400X).

Figure 4.28. Optical microscopy images of S14 (a) 200X and (b) 400X.

Sample S15 was prepared by water removal with 2 grams of silica particles in Reb A saturated 90 % ethanol. It was observed that the crystals formed were plates and rods in different sizes (Figure 4.29).
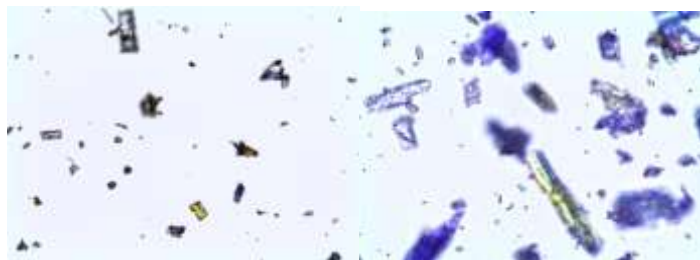

Figure 4.29. Optical microscopy images of S15 (400X).

Sample S16 (Figure 4.30) was prepared by adsorption of water by silica beads in 80% ethanol saturated with Reb A. Powder was found to contain short and wide particles as well as small rounded particles in varying sizes.

Figure 4.30. Optical microscopy images of S16 (400X).

The sample (S17), prepared by using 2 grams of silica particles in Reb A saturated 80 % ethanol, was observed to occur in crystals of various sizes with a very wide particle size distribution (Figure 4.31).
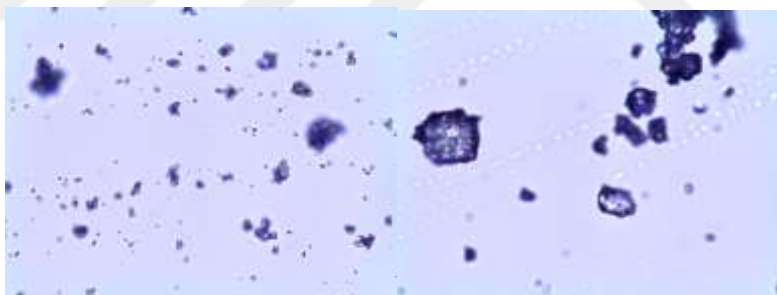
Figure 4.31. Optical microscopy images of S17 (a) 200X and (b) 400X.

4.2.3. Seed Crystals Prepared by Precipitation Method

Reb A is soluble in water but is insoluble in acetone. Preparation of Reb A seeds by precipitation was employed to obtain crystals having a narrow particle size distribution.

The optical microscopy images of the powder obtained by adding acetone dropwise to the saturated Reb A solution in water (Sample S19) are shown in Figure 4.32. The resulting crystals were large and the particle size distribution was wide. It was observed that the sample S20 had small and homogeneous crystals (Figure 4.33).
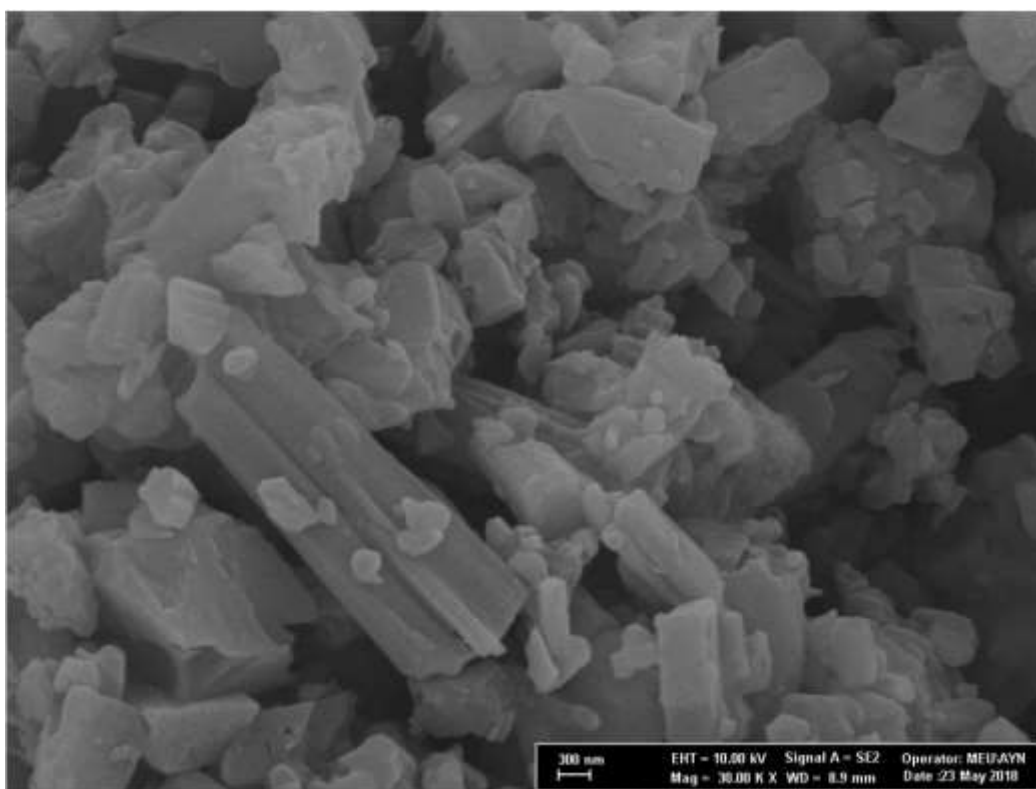

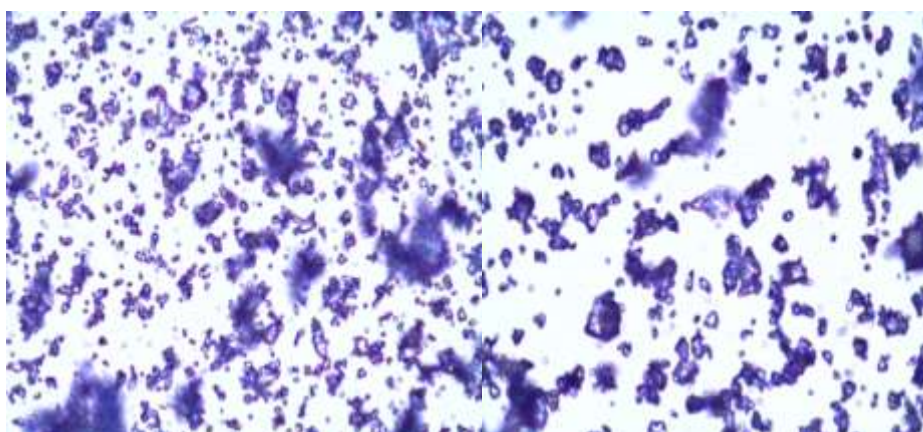**Figure 4.32.** Optical microscopy images of S19 (400X).

Figure 4.33. Optical microscopy images of S20 (400X).

Scanning electron microscopy was used in order to determine particle morphology and size in

detail for the selected samples. Figure 4.34 shows the SEM micrograph of the sample S20. The presence of small particles together with large rods and sphere-like particle showed that the sample had a wide particle size distribution. Optical microscopy images of the sample S21 (400X) and optical microscopy images of Sample S22 (400X) are given in Figure 4.35 and Figure 4.36, respectively.

Figure 4.34. SEM image of S20.

Figure 4.35. Optical microscopy images of S21 (400X).
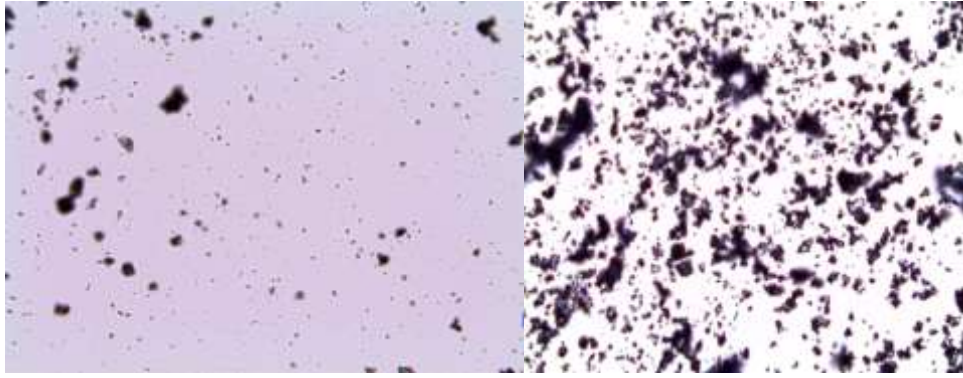
Figure 4.36. Optical microscopy images of S22 (400X).

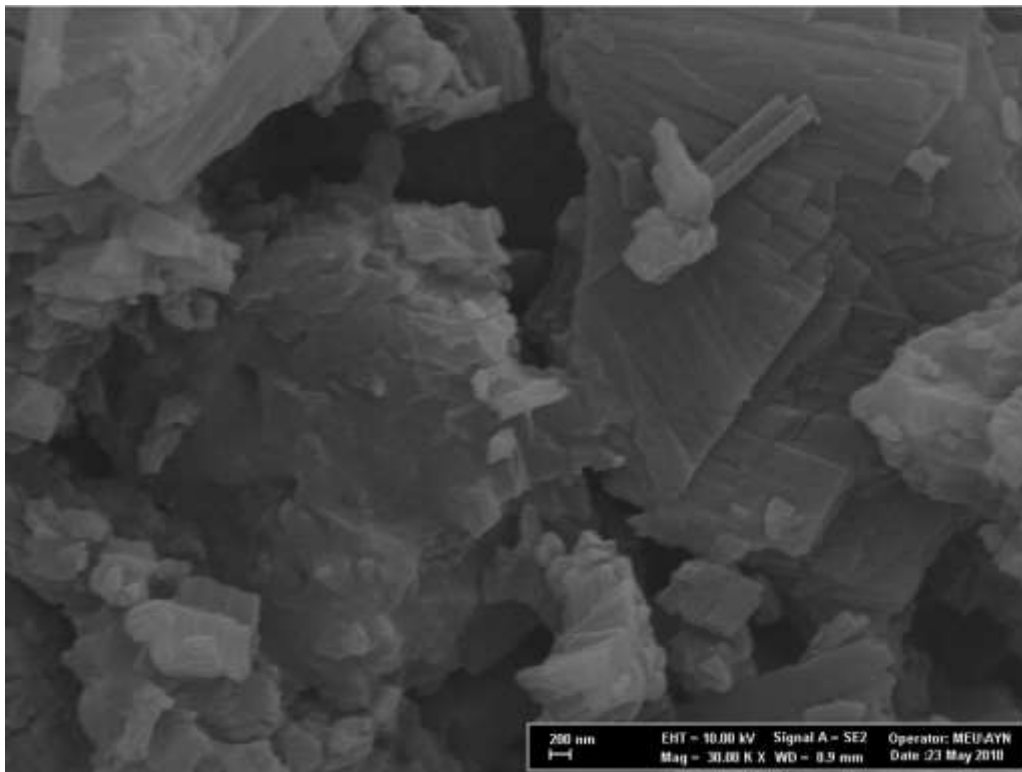The sample S21 however had very large plates composed of fused particles (Figure 4.37) whereas S22 consisted of small, large and relatively very large particles (Figure 4.38).

Figure 4.37. SEM image of S21.
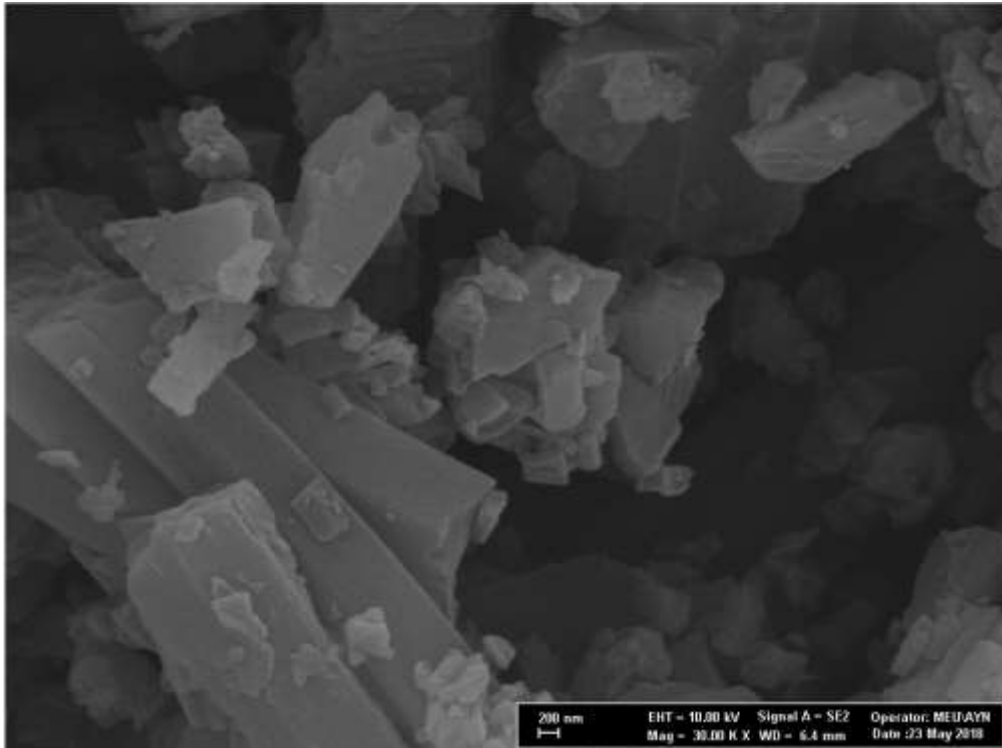
Figure 4.38. SEM image of S22.

Another sample prepared by precipitation (S23) had smaller crystals with a narrow size distribution (Figure 4.39) according to optical microscopy. Particle size distribution of this sample showed that volume median particle size was 34 µm. This indicated that powder with particles is larger than particles of Reb A starting powder were prepared by precipitation. Particle size distribution of S23 is given in Figure 4.40.

Figure 4.39. Optical microscopy images of S23 (400X).
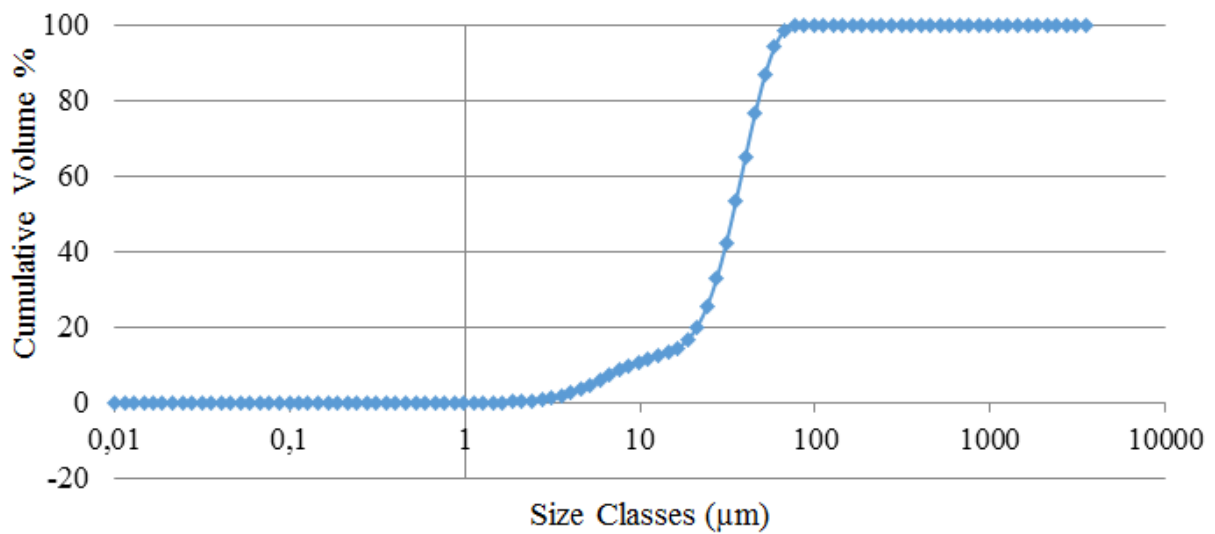
Figure 4.40. Particle size distribution of S23.

4.2.4. Seed Crystals Obtained by Dry Milling

The sample S24 prepared by grinding Reb A using zirconia balls was shown to consist of particles in similar sizes (Figure 4.41) hence a narrow particle size. SEM analysis however showed that the sample had very large particles formed by fusion of small particles (Figure 4.42). This may be related to the hardness of the particles of Reb A starting powder. Application of mechanical energy by milling using zirconia balls possibly deforms particles and fuse them together. Particle size distribution graph of S24 is given in Figure 4.43.
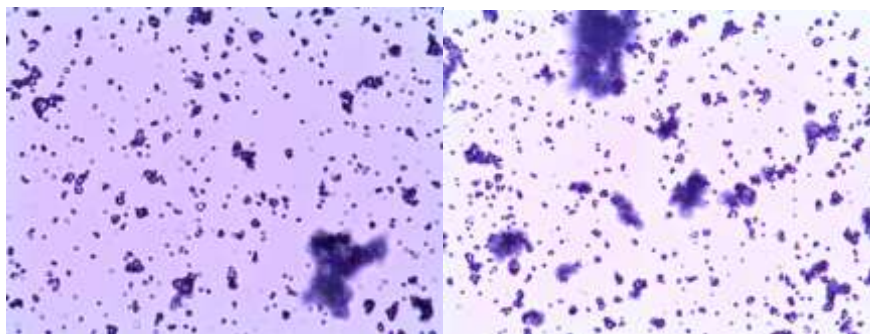
Figure 4.41. Optical microscopy images of S24 (400X).
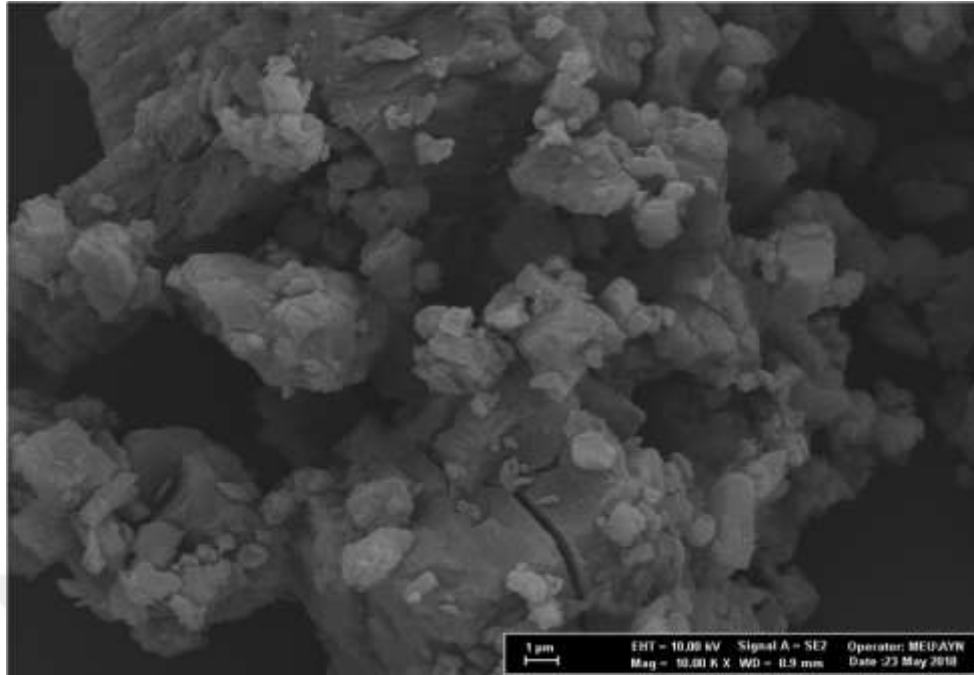
Figure 4.42. SEM image of S24.
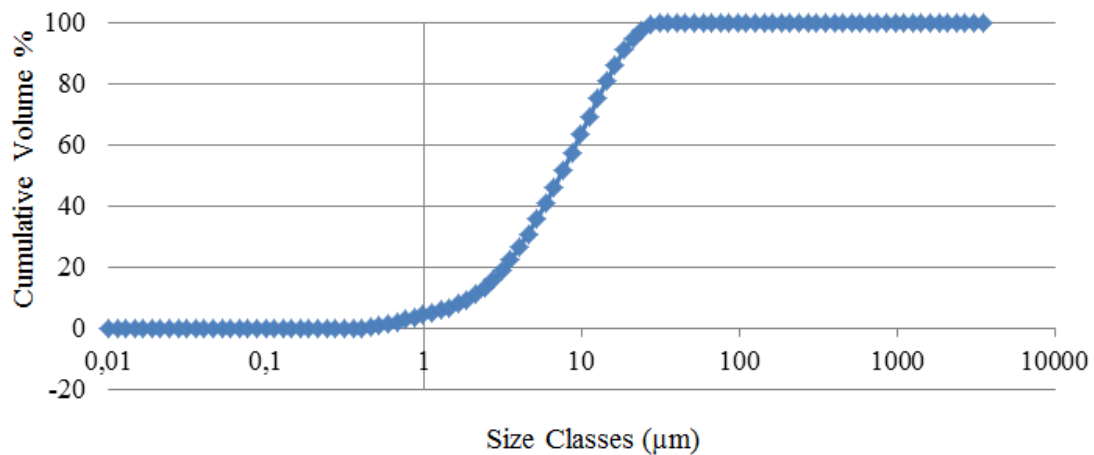
Figure 4.43. Particle size distribution graph of S24.

4.2.5. Seeds Prepared by Centrifugal Miller

Centrifugal miller was also employed to reduce the particle size and obtain a narrow particle size distirbution of Reb A starting powder. According to data obtained from Malvern Mastersizer, two methods resulted almost similar particle size distributions. One time milling showed slightly smaller volume median particle size than five times milling (11.5 and 13.2 μm for one time and five times milling, respectively). Particle size distribution graph of one

time centrifugall milling (S26) is given in Figure 4.44. Particle size distribution graph of five times centrifugall milling (S27) is given in Figure 4.45.
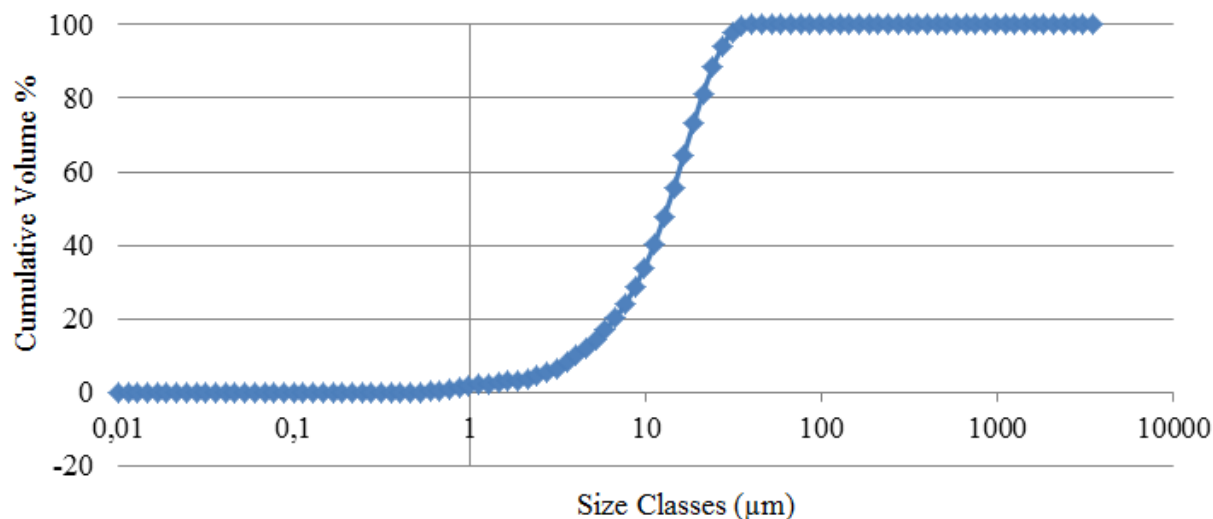
Figure 4.44. Particle size distribution graph of one time centrifugall milling (S26).
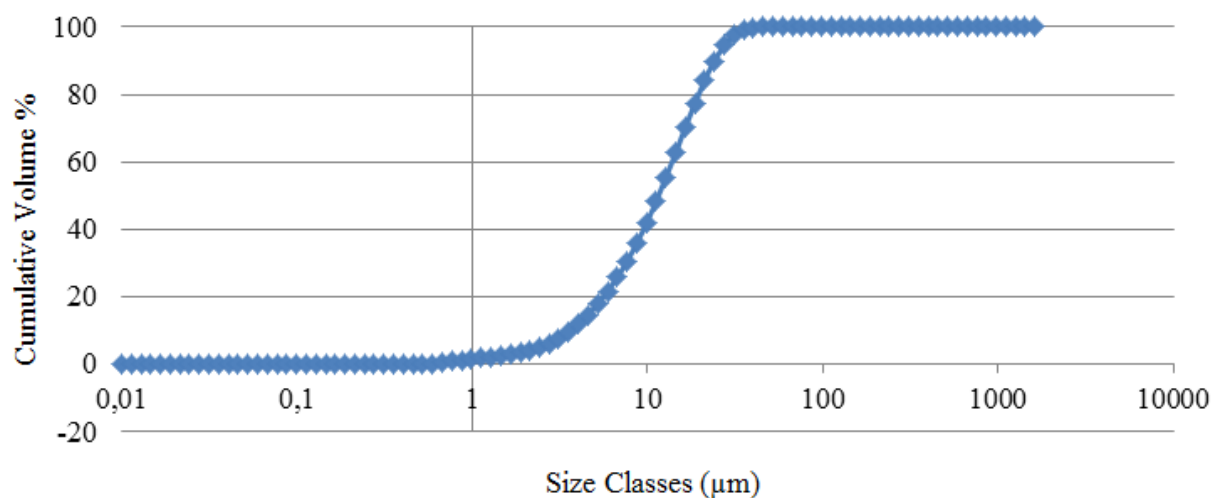
Figure 4.45. Particle size distribution graph of five times centrifugall milling (S27).

4.2.6. Seed Crystals Prepared by Crystallization at Constant Temperature

Reb A seed prepared by one time-centrifugal milling of starting powder (S26) was used in the determination of secondary nucleation tresholds of Reb A in water both in the static system and in the crystallization apparatus. Addition of seed to the saturated solutions resulted in the dissolution of the seed. Reb A seed was therefore prepared by crystallization at 60 °C from supersaturated Reb A solution. Resultant seed crystals were ground at 6000 rpm in the centrifugal miller and used in the secondary nucleation treshold experiments.

Crystal phases of Reb A starting powder and ground water grown Reb A crystals were determined by X-Ray diffraction analysis. XRD analysis of the powders showed that Reb A crystals grown in water had different crystal structure than Reb A starting powder (Figure 4.46). Grinding using centrifugal miller however resulted in the decrease of peak intensities indicating the reduction in the crystal sizes of the particles. XRD patterns together with optical images showed that phase transformation occurs in the supersaturated solutions of Reb A.
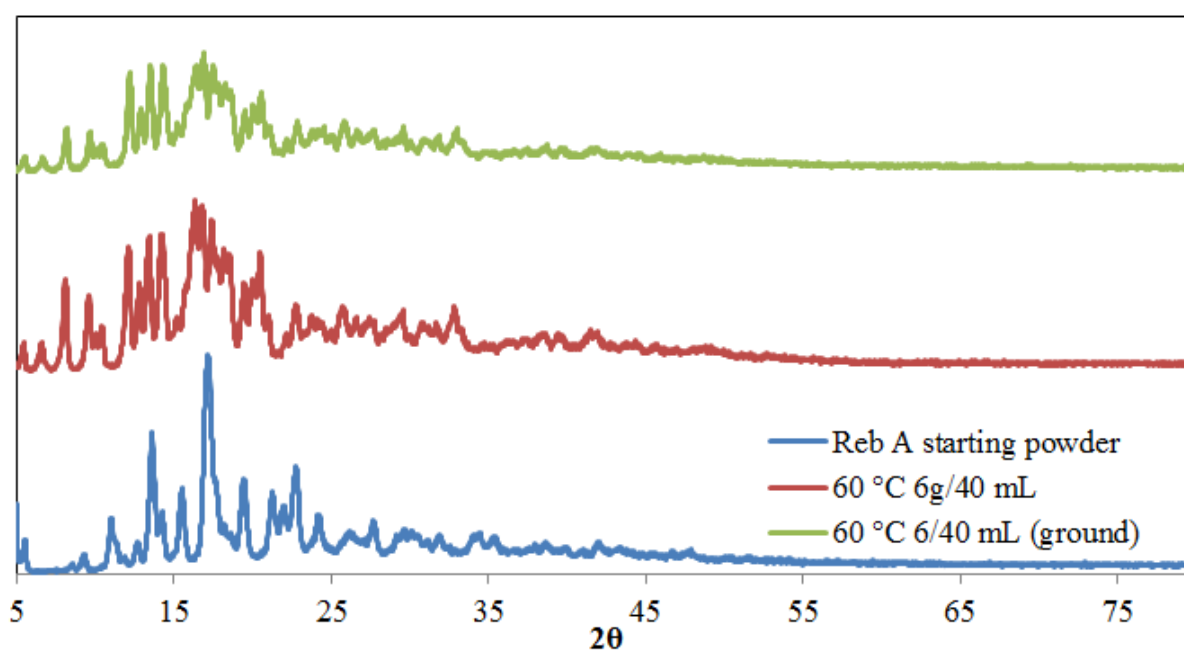
Figure 4.46. X-Ray diffraction patterns of Reb A starting powder and seed crystals.

4.3. Determination of Nucleation Thresholds in the Static System

The primary nucleation times and tresholds of Reb A in water at 25, 40, 50 and 60°C were determined by turbidity measurements. Figure 4.47 shows the primary nucleation times of the Reb A solutions in different solid to liquid ratios at 25°C. Nucleation started within 2 hours in solutions with high solid to liquid ratios. Turbidity of the Reb A solution with 0.0025 g/mL solid to liquid ratio was stayed constant throughout 12 hours of incubation. The nucleation treshold of Rebaudiside A was found to be between 0.0025 and 0.004 g/mL.
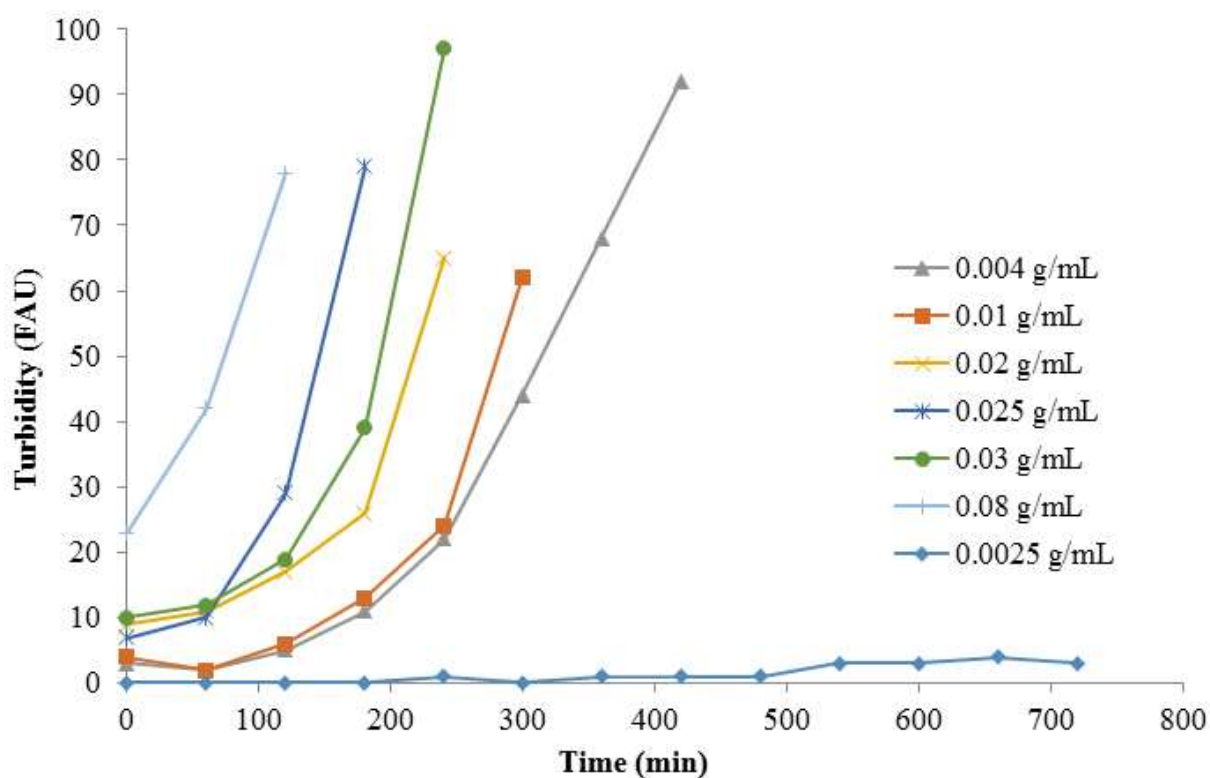
Figure 4.47. Turbidity values of Reb A aqueous solutions at 25 °C.

Turbidity values of Reb A solution incubated at 40 °C are given in Figure 4.48. Nucleation was observed to happen after 1 hour incubation at 40 °C when the solid to liquid ratio was 0.004 g/mL. No nucleation was observed in Reb A solutions with 0.001 and 0.0025 g/mL solid to liquid ratios within 10 hours of incubation. Primary nucleation treshold of Reb A in water was found to lay between 0.004 and 0.0025 g/mL.
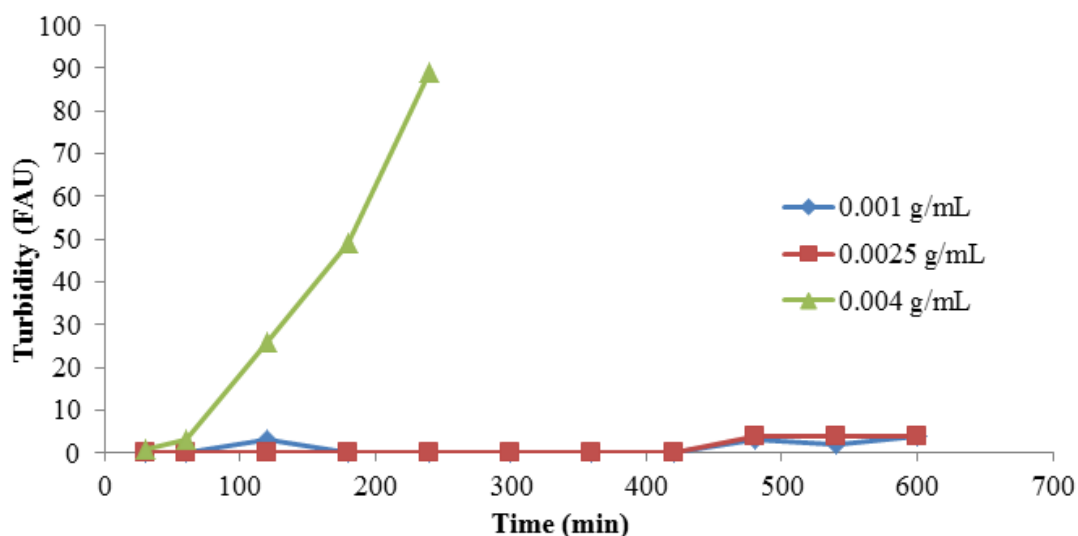
Figure 4.48. Turbidity values of Reb A aqueous solutions at 40 °C.

The primary nucleation times obtained by turbidity measurement at 50 °C are given in Figure 4.49. Primary nucleation threshold at this temperature was found to be between 0.01 and 0.004 g/mL. The primary nucleation threshold at 60 °C was also found to be between 0.01 and 0.004 g/mL (Figure 4.50). Nucleation started after 2 hours at 50 °C but after 1 hour at 60 °C showing that 10 °C increase in temperature does not increase nucleation terskhold significantly but increases the rate of nucleation. When the primary nucleation treshold of Reb A at 50 and 60 °C was compared to those at 25 and 40 °C, it was observed that the increase in temperature increased the nucleation treshhold. This is possibly due to the higher solubility of Reb A in water at higher temperatures.
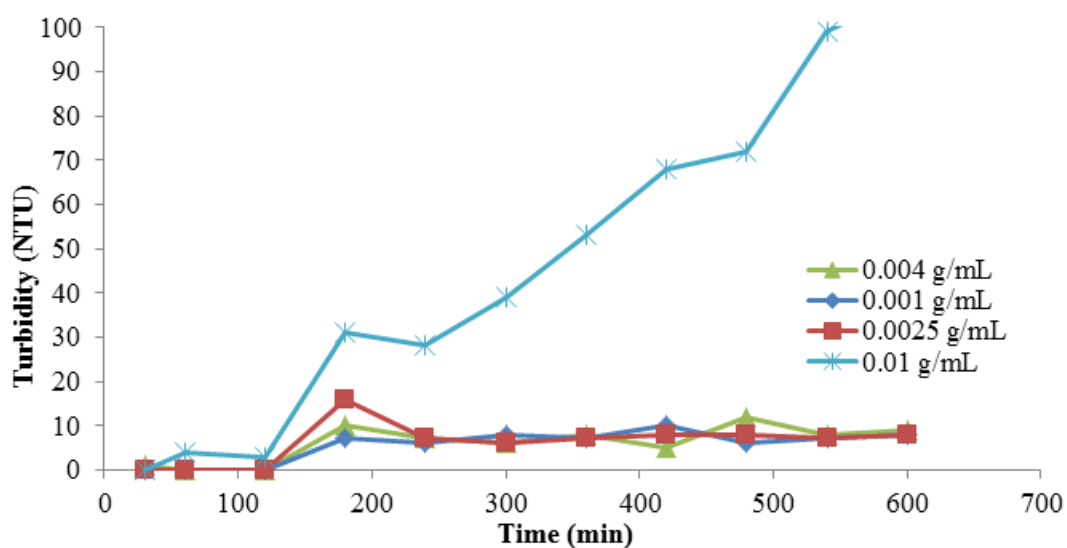
Figure 4.49. Turbidity values of Reb A aqueous solutions at 50 °C.
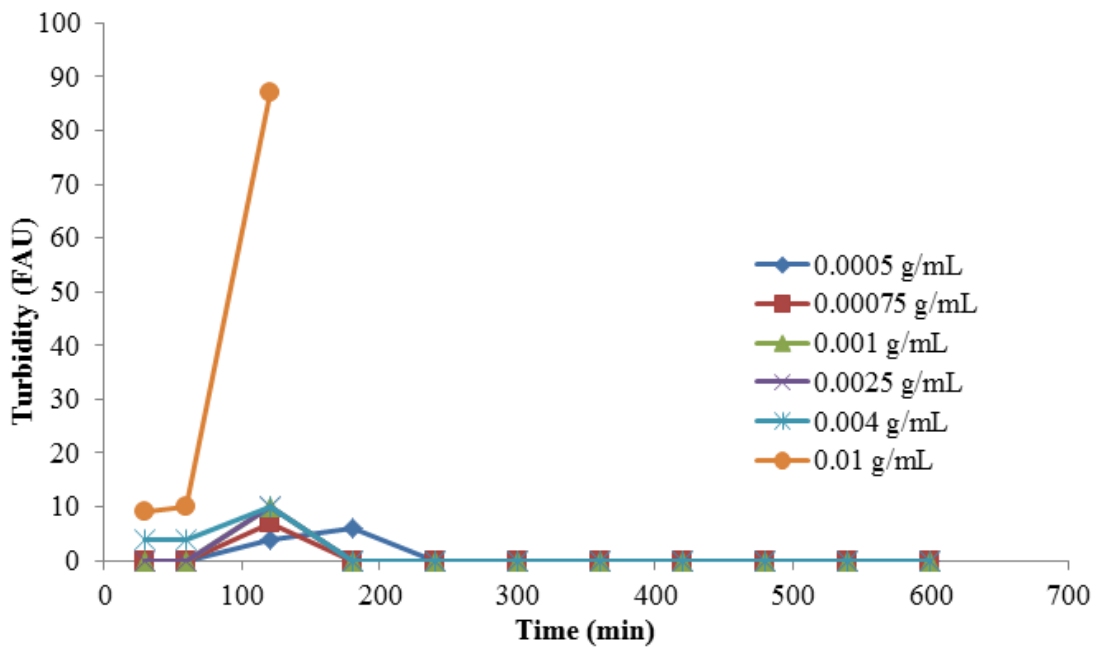
Figure 4.50. Turbidity values of Reb A aqueous solutions at 60 °C.

4.4. Determination of Primary Nucleation in the Stirred Reactor

Statically determined primary nucleation treshholds were used to determine nucleation treshold in stirred sytem. After a series of experiments, primary nucleation thresholds could only be determined for 30 and 40 °C since experiments at 50 °C yielded inconsistent results due to the evaporation of water from the Reb A solutions. The determination of nucleation was performed by visual inspection. The highest solid to liquid ratios in which the nucleation was detected were 0.0040 and 0.00475 g/mL for 30 and 40 °C, respectively (Table 4.3).

Table 4.3. Primary nucleation tresholds in the reactor.

30 °C		40 °C	
Solid/liquid ratio g/mL	Nucleation occurance	Solid/liquid ratio g/mL	Nucleation occurance
0.0040	+	0.0047	-
0.0039	-	0.00474	-
0.0038	-	0.00475	+
0.0037	-	0.0048	+
		0.0049	+
		0.0051	+
		0.0055	+

4.5. Secondary Nucleation Threshold in Static System

Secondary nucletion tresholds of Reb A in water at 20, 30 and 40°C were determined by the addition of seed (A1) suspension into Reb A solution with different solid-liquid ratios incubated in constant temperature water bath. The visual appearence of the samples used in the determination of secondary nucleation treshold at 20°C is given in Figure 4.51.
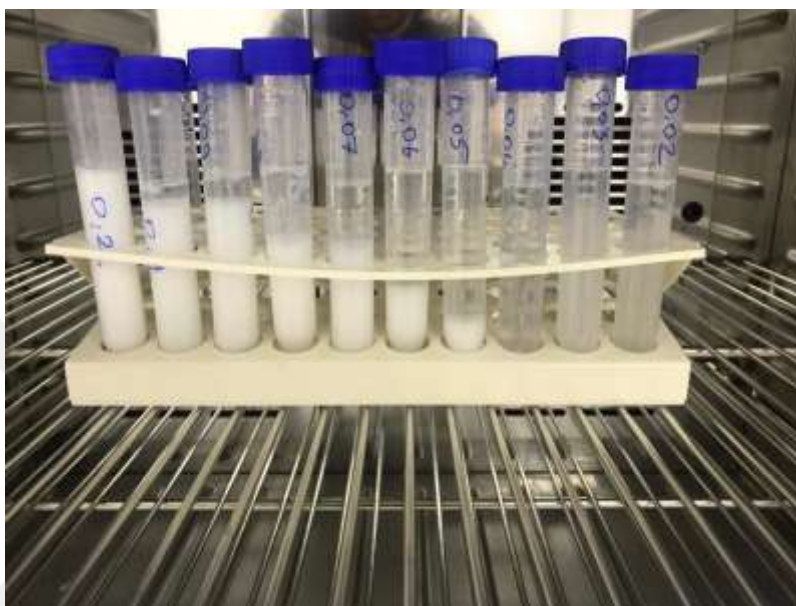
Figure 4.51. The secondary nucleation treshold at 20°C.

Secondary nucleation tresholds of Reb A in water are shown in Table 4.4. Secondary nucleation treshold at 20 °C was determined to be between 0.002 and 0.003 g/mL whereas those at 30 and 40 °C were between 0.003 and 0.004 g/mL.

Table 4.4. Secondary nucleation thresholds of Reb A.

| Solid to Liquid Ratios (g/mL)	Temperature (°C)		
	20	**30**	**40**
0.02	+	+	+
0.01	+	+	+
0.008	+	+	+
0.007	+	+	+
0.006	+	+	+
0.005	+	+	+
0.004	+	+	+
0.003	+	-	-
0.002	-	-	-
0.001	-	-	-
0.00045	-	-	-

4.6. Isothermal Crystal Growth of Reb A

Secondary nucleation treshold determinations were performed during isothermal growth of Reb A in water. Experiments were restricted to the temperatures of 20, 30 and 40 °C due to the solvent evaporation at and above 50 °C. Since the secondary nucleation treshold of Reb A at 20 °C was determined to be betweeen 0.002 and 0.003 g/mL in static system, 0.0025 g/mL was used in the isothermal crystal growth experiments at 20 °C. When the solid liquid ratio was used as 0.0025 g/mL, secondary nucleation could not be observed within 96 hours. Similarly, when solid to liquid ratio was increased to 0.004 g/mL, it was not possible to observe nucleation. Further increase in solid to liquid ratio exhibited both nucleation and crystal growth. Any nucleation could not be detected for three different solid to liquid ratios at 30 °C and one solid to liquid ratio at 40 °C.

Table 4.5. Secondary nucleation treshold of Reb A at 20 °C, 30 °C, and 40 °C.

20 °C		30 °C		40 °C	
g/mL	Nucleation	g/mL	Nucleation	g/mL	Nucleation
0.0025	-	0.003	-	0.035	-
0.004	-	0.0035	-		
0.01	Nucleation + Crystal growth	0.0055	-		

It was not easy to observe secondary nucleation thresholds visually in the stirred reactor. Turbidity caused by the addition of seed interfered with the turbidity resulting from the nucleation. Concentration of Reb A however was measured to determine the presence of secondary nucleation. Visual inspection combined with absorbance measurement showed that only one solid to liquid ratio (0.001 g/mL) at 20 °C showed both nucleation and crystal growth. Absorbance values of samples collected from the reactor throughout 120 hours crystallization experiment are shown in Figure 4.52. Absorbance values decreased during 96 hours and stayed constant thereafter until 120th hour.
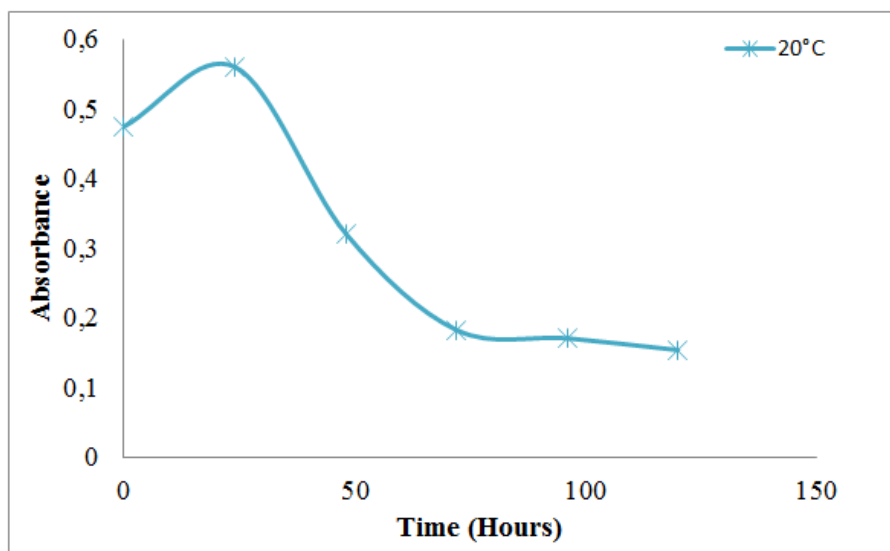
Figure 4.52. Absorbance change in the samples taken during isothermal crystal growth experiment at 20°C.

5. CONCLUSIONS

The use of natural low-calory sweeteners in food industry has become inevitable due to the increasing awareness on human health. Cultivation of stevia has spreaded all over the world but the production technology of high purity steviol glycosides is still advancing. The measurement of solubilities of steviol glycosides in various solvents and their temperature dependence significantly contributes to their extraction, separation and purification. Investigation of their crystallization behavior also makes it possible to produce high purity steviol glycosides with desired properties via crystallization. In this respect, the crystallization of Reb A in water was investigated in this thesis. Solubility of Reb A in water was first determined at different temperatures. Solubility values of Reb A in water at 40, 50 and 60 °C were found to be 3.94, 5.93 and 10.65 mg Reb A/g water, respectively.

Reb A is known to have different polymorphs and different Reb A crystal phase with lower water solubility grows from the supersaturated solutions. This was confirmed by optical microscopy and X-ray diffraction analysis in this thesis. Water grown Reb A crystals was found to be long but thin whisker like crystals indicating a one-dimensional crystal growth. Temperature dependent solubility values of water grown Reb A crystals were measured to be 0.55, 0.52, 0.70, 4.53 and 7.87 mg Reb A/g water at 20, 30, 40, 50 and 60 °C, respectively. Primary and secondary nucleation thresholds of Reb A in water were determined by both statically and in the stirred reactor based on the solubility data of Reb A starting powder and water grown Reb A crystals. For the determination of secondary nucleation thresholds, Reb A seeds were produced by various methods and characterized in terms of their particle morphology and size distribution. A seed prepared by grinding of water grown Reb A crystals was selected to be used in the secondary nucleation experiments. Primary nucleation tresholds lay between 0.0025 and 0.004 g/mL for 25 and 40 °C and between 0.004 and 0.01 g/mL for 50 and 60 °C when measured statically. Primary nucleation tresholds were measured as 0.00399 g/mL and 0.00474 g/mL for 30 and 40 °C, respectively in the strired reactor. Secondary nucleation experiments in the static system showed that the secondary nucleation tresholds were between 0.002 and 0.003 g/mL for 20 °C and 0.004 and 0.003 g/mL for 30 and 40 °C, respectively. Seondary nucleation tresholds could not be determined by isothermal crystal growth experiments since it was not possible to detect nucleation clearly due to the turbidity caused by the addition of seed suspension with the amount of seed suspension used in this study.

6. RECOMMENDATIONS

Based on the results obtained in this thesis, some future prospects can be summarized below.

- Because crystallization experiments are prone to personal errors, if possible, the use of Focused Beam Reflectance Measurement (FBRM), Attenuated Total Reflectance-Fourier Transform Infrared Spectroscopy (ATR-FTIR) or turbidity probes for in line detection of nucleation are strongly suggested.

- Crystallization and solubility experiments can be performed at temperatures other than those used in this thesis especially at temperature between 4 and 20 °C.

- Solubility of Reb A starting powder and water grown Reb A crystals can be measured at various pH values.

- Nucleation kinetics of Reb A in water can be measured.

- Nucleation and crystallization behaviour of Reb A in different ethanol-water mixtures can be performed.

- The behavior of Reb A in water at temperatures ≥ 70 °C should be studied in details.

REFERENCES

Abou-Arab, A. E., Abou-Arab, A. A., & Abu-Salem, M. F. (2010). Physico-chemical assessment of natural sweeteners steviosides produced from Stevia rebaudiana Bertoni plant. *African Journal of Food Science*, *4*(5), 269-281.

Alvarez, A. J., & Myerson, A. S. (2010). Continuous plug flow crystallization of pharmaceutical compounds. *Crystal Growth & Design*, *10*(5), 2219-2228.

Beckmann, W. (Ed.). (2013). *Crystallization: basic concepts and industrial applications*. John Wiley & Sons.

Beiny, D. H. M., & Mullin, J. W. (1987). Solubilities of higher normal alkanes in m-xylene. *Journal of Chemical and Engineering Data*, *32*(1), 9-10.

Berk, Z. (2018). *Food process engineering and technology*. Academic press.

Brahmachari, G., Mandal, L. C., Roy, R., Mondal, S., & Brahmachari, A. K. (2011). Stevioside and related compounds–molecules of pharmaceutical promise: a critical overview. *Archiv der Pharmazie*, *344*(1), 5-19.

Carbone, M. N., & Etzel, M. R. (2006). Seeded isothermal batch crystallization of lysozyme. *Biotechnology and bioengineering*, 93(6), 1221-1224.

Celaya, L. S., Kolb, E., & Kolb, N. (2016). Solubility of Stevioside and Rebaudioside A in water, ethanol and their binary mixtures. *International Journal of Food Studies*, *5*(2), 158-166.

Çetin, A. E., Kola, O., & Özer, M. S. (2015). Determination of the solubility values of Rebaudioside A produced from steviol glucosydes having natural sweetener ability specified from stevia rebaudiana bertoni. *Adana Science and Technology University*, MÜHDBF.GIDA.2015-9.

Çetin, A. E., Kola, O., Yurtsever, H. A., İpek, S. L., Cengiz, N. (2017). Determination of crystallization kinetics of Rebaudioside A. *Adana Science and Technology University*, 17103005.

Decloux, M., 2002. Crystallisation. In: Bimbenet, J.J., Duquenoy, A., Trystram, G. (Eds.), *Genie des Procedes Alimentaires*, (pp. 179–194). Dunod, Paris.

FAO/WHO. (2017). Retrieved from http://www.fao.org/3/BU297en/bu297en.pdf.

Gao, Z., Rohani, S., Gong, J., & Wang, J. (2017). Recent developments in the crystallization process: toward the pharmaceutical industry. *Engineering*, *3*(3), 343-353.

GRAS Assessment, Layn Corp. (2010). Rebaudioside A (≥97%), Food usage conditions for general recognition of safety For Guilin Layn Natural Ingredients Corp., Guilin, China. Retrieved from http://wayback.archive-it.org/7993/20171031045739/https://www.fda.gov/downloads/Food/IngredientsPackagingLabeling/GRAS/NoticeInventory/UCM269561.pdf.

Hartel, R. W. (2001). *Crystallization in foods*. Aspen Publishers.

Jouppila, K., & Roos, Y. H. (1994). Glass transitions and crystallization in milk powders. *Journal of Dairy Science*, *77*(10), 2907-2915.

Lemus-Mondaca, R., Vega-Gálvez, A., Zura-Bravo, L., & Ah-Hen, K. (2012). Stevia rebaudiana Bertoni, source of a high-potency natural sweetener: A comprehensive review on the biochemical, nutritional and functional aspects. *Food chemistry*, *132*(3), 1121-1132.

Kinghorn, A. D. (2002). *Stevia: The Genus Stevia*, Taylor & Francis, London.

Mersmann, A. (Ed.). (2001). *Crystallization technology handbook*. (2nd ed.). CRC Press.

Miers, H. A. & Isaac, F. (1906). Refractive indices of crystallizing solutions. *Journal of the Chemical Society*, *89*, 413-454.

Miers, H. A. & Isaac, F. (1907). The spontaneous crystallization of binary mixtures. *Proceedings of the Royal Society*, *A79*, 322-351.

Mullin, J. W. (2001). *Crystallization*. Reed Educational and Professional Publishing Ltd.

Myerson, A. (2001). *Handbook of industrial crystallization*. Butterworth-Heinemann.

Prakash, I., DuBois, G. E., King, G. A., Upreti, M. (2007). Rebaudioside A composition and method for purifying Rebaudioside A. Patent Application Publication. Pub. No.: US 2007/0292582 A1.

Prakash, I., Markosyan, A., & Bunders, C. (2014). Development of next generation stevia sweetener: Rebaudioside M. *Foods*, *3*(1), 162-175.

Prakash, I., Clos, J. F., & Chaturvedula, V. S. P. (2012). Stability of Rebaudioside A under acidic conditions and its degradation products. *Food Research International*, *48*(1), 65-75.

Prakash, I., DuBois, G. E., Clos, J. F., Wilkens, K. L., & Fosdick, L. E. (2008). Development of rebiana, a natural, non-caloric sweetener. Food and Chemical Toxicology, *46*(7), S75-S82.

Prausnitz, J. M., Lichenthaler, R. N., & Gomes de Azevedo, E. G. (1999). *Molecular thermodynamics of fluid-phase equilibria*, 3rd ed., Prentice- Hall. Inc.

Rashid, M. A. (2011). *Crystallization engineering of Ibuprofen for pharmaceutical formulation*. Doctorial Thesis. The University of Queensland.

Puri, M., Sharma, D., & Tiwari, A. K. (2011). Downstream processing of stevioside and its potential applications. *Biotechnology Advances*, *29*(6), 781-791.

Saikumar, M. V., Glatz, C. E., & Larson, M. A. (1998). Lysozyme crystal growth and nucleation kinetics. *Journal of crystal growth*, 187(2), 277-288.

Tavare, N. S. (1995). *Industrial crystallisation: Process simulation analysis and design*. Plenum Press, New York.

Tung, H.-H., Paul, E. L., Midler, M., & McCauley, J. A. (2009). *Crystallization of organic compounds: an industrial perspective*. John Wiley & Sons.

Upreti, M., Smit, J. P., Hagen, E. J., Smolenskaya V. N., & Prakash, I. (2012). Single crystal growth and structure of the natural "High Potency" sweetener Rebaudioside A". *Crystal Growth and Design*, *12*(2), 990-993.

Wölwer-Rieck, U. (2012). The leaves of Stevia rebaudiana (Bertoni), their constituents and the analyses thereof: a review. *Journal of Agricultural and Food Chemistry*, *60*(4), 886-895.

Zhao, H.-Y., Gu, Z.-B., Cheng, L., L1, Z.-F., & Hong, Y. (2012). Determination of solubility and supersolubility of Rebaudioside A in methanol aqueous solution. Science and Technology of Food Industry, (11).
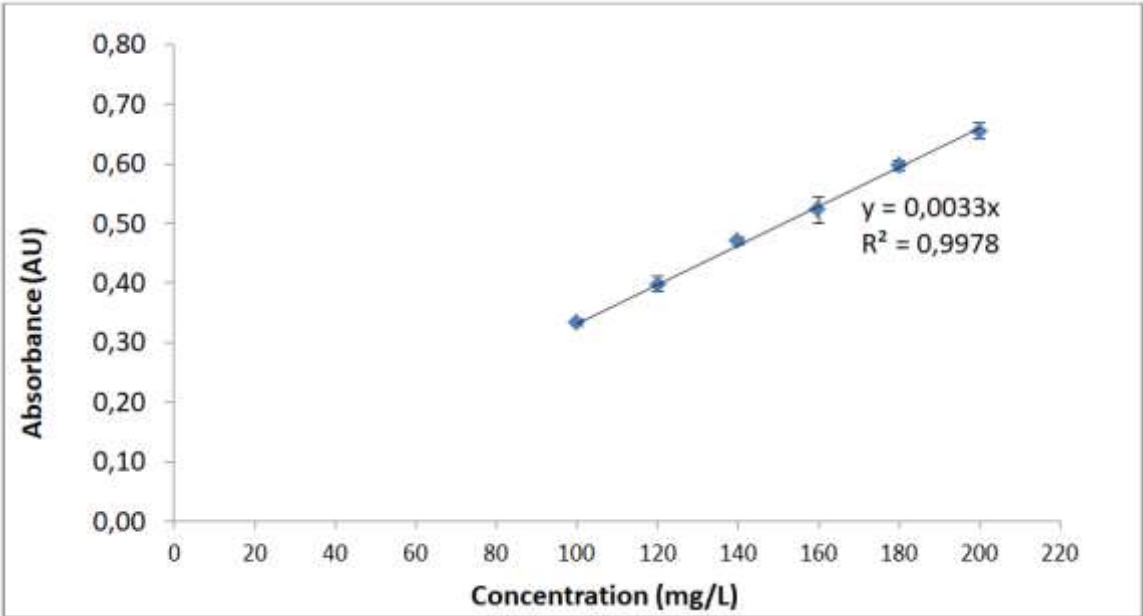
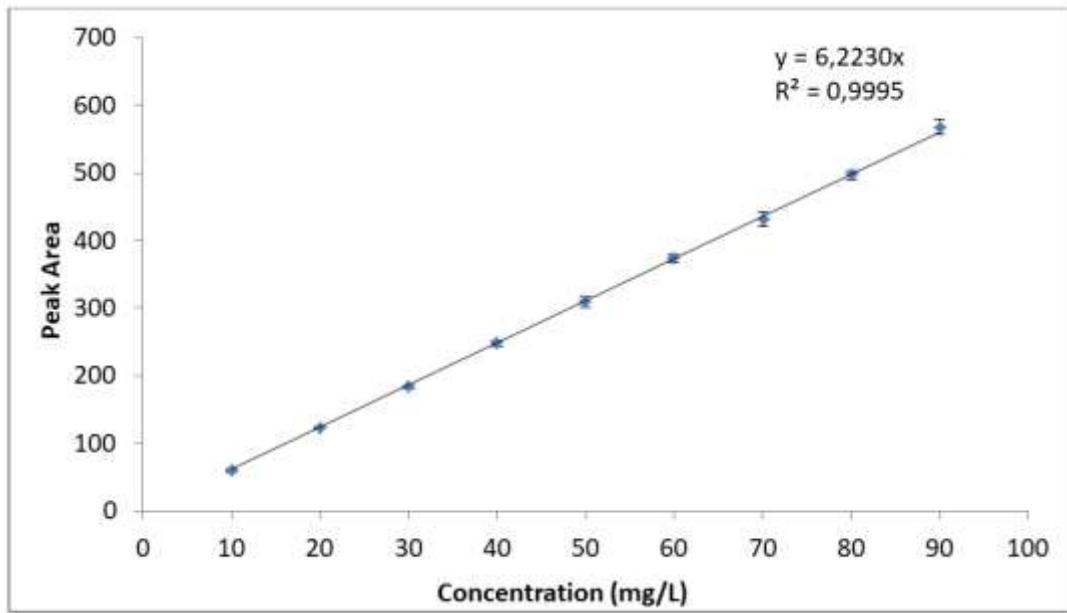# APPENDICES

APPENDIX A1
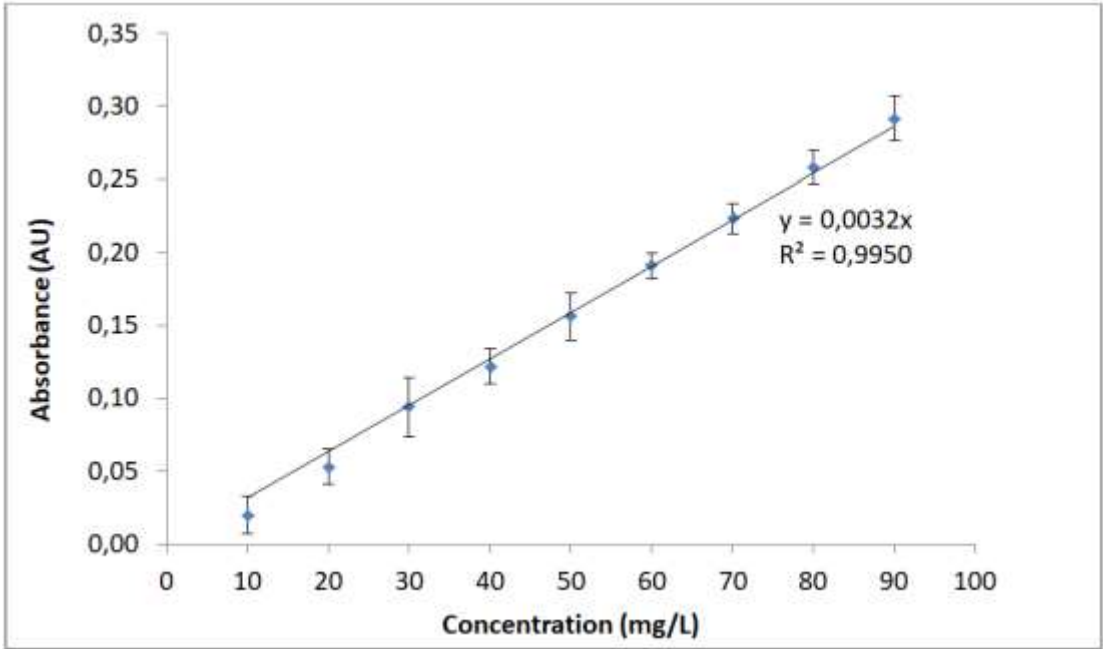
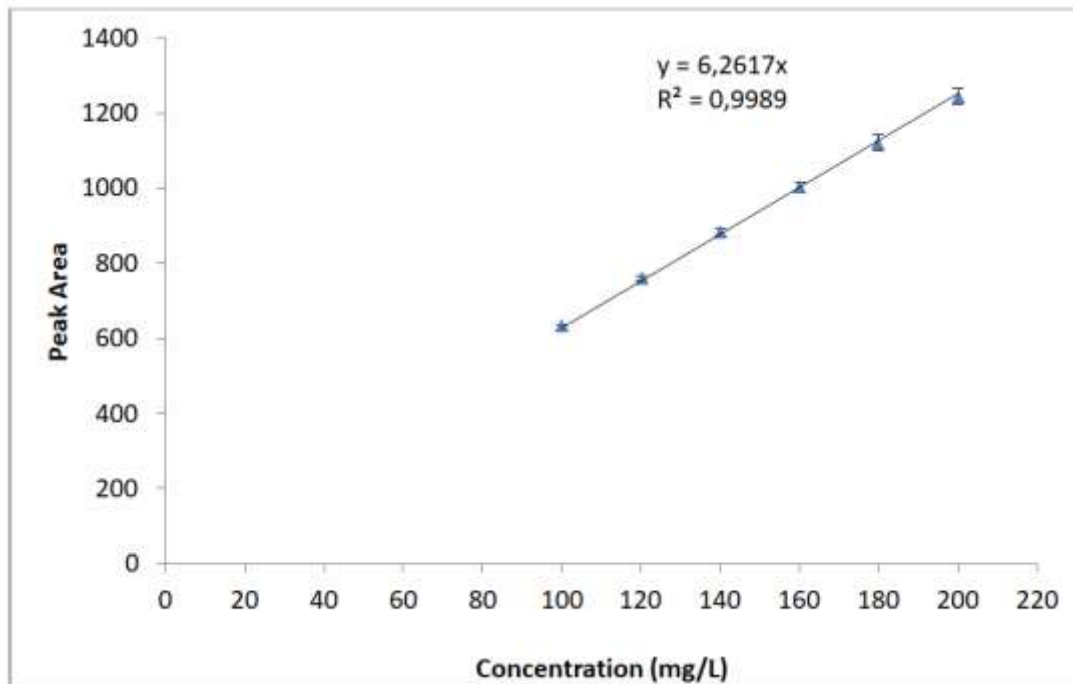

Figure A1.1- Calibration curves obtained for 10-90 mg/L concentration range by UV-Visible spectrophotometry.

Figure A1.2- Calibration curves obtained for 100-200 mg/L concentration range by UV-Visible spectrophotometry.
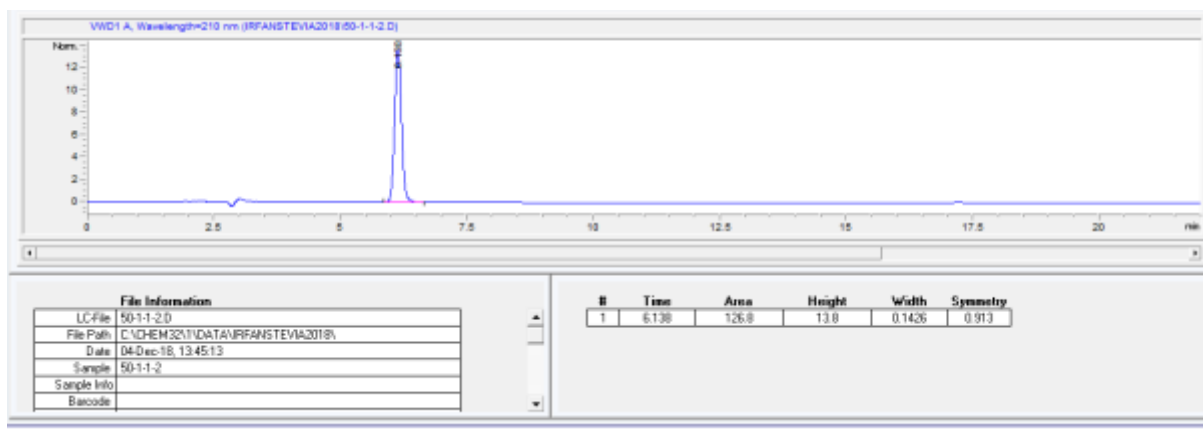
Figure A1.3- Calibration curve obtained for 10–90 mg/L concentration range by HPLC (Injection volume: 20 µL).
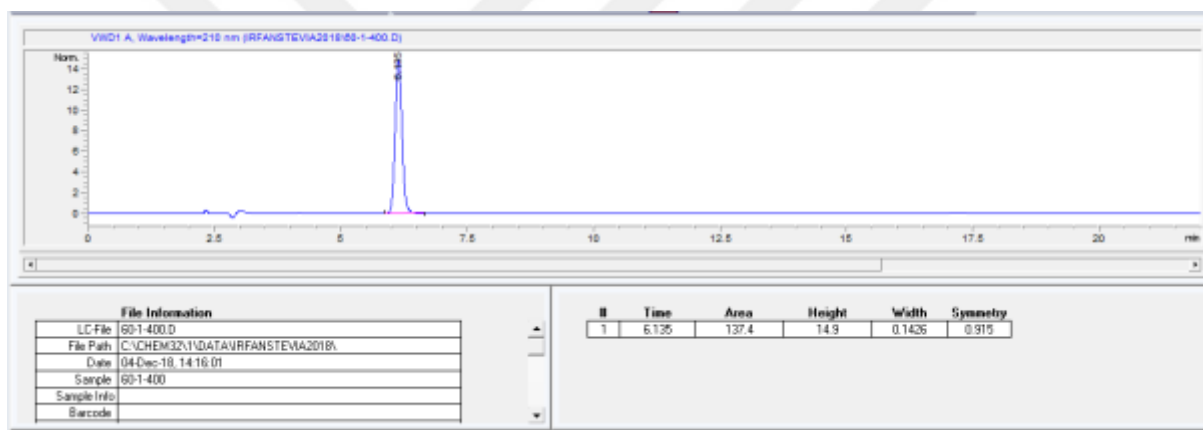

Figure A1.4- Calibration curve obtained for 100–200 mg/L concentration range by HPLC (Injection volume: 20 µL).
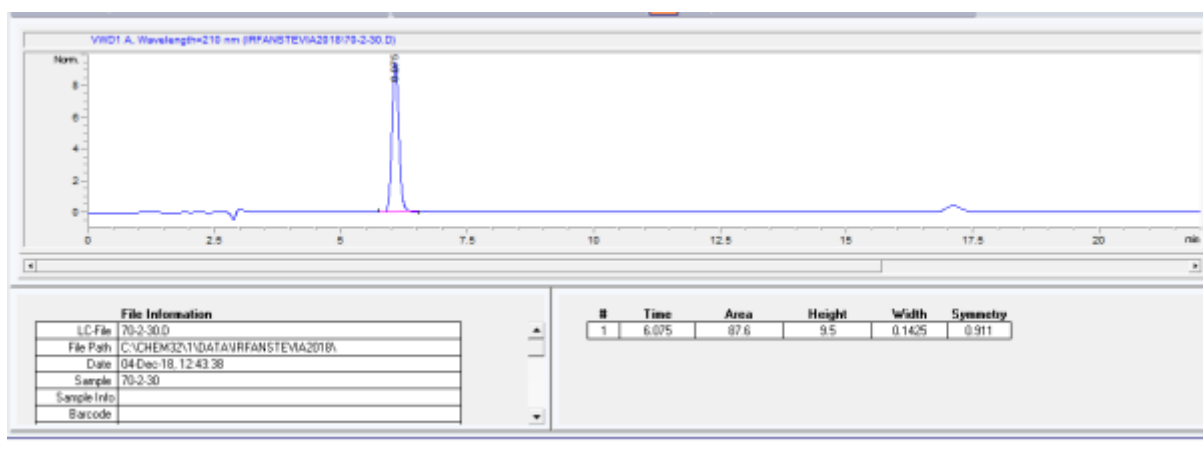
APPENDIX A2

Figure A2.1 HPLC chromatogram of sample prepared by diluting Reb A solution incubated at 50 °C.

Figure A2.2 HPLC chromatogram of sample prepared by diluting Reb A solution incubated at 60 °C.

Figure A2.3 HPLC chromatogram of sample prepared by diluting Reb A solution incubated at 70 °C.

CURRICULUM VITAE

PERSONEL INFORMATION

Name Surname	: Semih Latif İpek
Contact Number	: (0322) 455 00 00 - 2093
Mail	: slipek@atu.edu.tr

EDUCATION

Master of Science :	: Adana Alparslan Türkeş Science and Technology University (2016-present) *Graduate School of Natural and Applied Science* *Food Engineering Department*
Bachelor of Science	: Gaziantep University (2006-2013) *Faculty of Engineering* *Food Engineering Department*